Fluid-Phase Equilibrium Experiments and Modeling for CO 2 + C 6 Binary Systems

Sergiu Sima, Catinca Secuianu, Dan Vladimir Nichita

Fluid Phase Equilibria Experiments and Modeling for CO_2 + C_6 binary systems

Sergiu Sima,[1] Catinca Secuianu[1*], and Dan Vladimir Nichita[2,*]

[1]*Department of Inorganic Chemistry, Physical Chemistry and Electrochemistry, Faculty of Chemical Engineering and Biotechnologies, National University of Science and Technology POLITEHNICA Bucharest, 1-7 Gh. Polizu Street, S1, 011061 Bucharest, Romania, catinca.secuianu@upb.ro;*

[2]*CNRS UMR 5150, Laboratoire des Fluides Complexes et leurs Réservoirs, Université de Pau et des Pays de l'Adour, B.P. 1155, 64013, Pau Cedex, France; tel. +33-0716750935, e-mail: dnichita@univ-pau.fr*

ABSTRACT:

The phase behavior of the carbon dioxide and *n*-hexane binary mixture was examined. The entire available literature was reviewed and analyzed. Despite the apparent abundance of experimental data – both vapor–liquid equilibrium (VLE) and critical data, there is a high degree of discrepancy between them. Therefore, the liquid–vapor critical line was determined up to 117.0 bar and 383.15 K, as well as vapor–liquid equilibrium (VLE) data at different constant temperatures (313.15 to 383.15 K) using a 60 cm^3 stainless steel cell with sapphire windows connected to a gas chromatograph via rapid online sample injectors – ROLSI valves for accurate compositions detection. The new and literature data were successfully calculated with several models (**G**eneral **E**quation **O**f **S**tate – GEOS, Peng–Robinson – PR, Soave–Redlich–Kwong – SRK), in association with classical van der Waals mixing rules, i.e., one- (1PCMR) and two-parameter conventional (2PCMR) combining rules, as well as PPR78 model. We also studied the influence of the structure of organic compounds (*n*-alkane, cycloalkane, and branched alkane – position isomer) with the same number of carbon atoms on the phase behavior of their corresponding binary systems at high pressures.

1. INTRODUCTION

Carbon dioxide (CO_2) and *n*-hexane (n-C_6H_{14}) binary system has attracted significant attention in both academic and industrial research due to its interesting thermodynamic and phase

*Corresponding authors: catinca.secuianu@upb.ro (C. Secuianu), dnichita@univ-pau.fr (D.V. Nichita)

behavior.[1,2,3,4,5,6] *n*-Hexane is a non-polar molecule that exhibits unique interactions with CO_2, a polar molecule, leading to the formation of complex phase equilibria and intermolecular forces within the mixture. Understanding the phase behavior of these binary systems is crucial in various fields such as chemical, oil, and materials engineering, environmental science, extraction and purification processes, carbon capture and storage (CCS), process optimization, food and beverage processing, chemical and pharmaceutical synthesis, as well as in applications like gas extraction, separation processes, and enhanced oil recovery (EOR), etc.[7,8,9,10,11,12,13,14] For instance, CO_2 flooding is a well-established technique in the oil and gas sector. The viscosity of crude oil is lowered, its mobility is improved, and it is displaced toward production wells by the injection of CO_2, often in conjunction with *n*-hexane, into oil reservoirs.[15,16] Enhanced sweep efficiency and ultimately increased oil recovery rates are a result of the CO_2 + *n*-hexane binary system's capacity to modify fluid characteristics and interact with reservoir fluids. The practice of capturing carbon dioxide from industrial sources, such power plants and refineries, is becoming more popular as the emphasis on reducing greenhouse gas emissions grows.[17,9] In solvent-based carbon capture procedures, CO_2 is selectively absorbed from flue gases by use of an appropriate solvent. Because of its compatibility and advantageous characteristics, *n*-hexane can increase the solvent's capacity to absorb CO_2, making it easier to separate and store or use the CO_2 that has been captured. The extraction and purification of natural products, such as essential oils, flavors, and fragrances, is one common use. Supercritical CO_2 extraction provides a clean and effective way to extract valuable compounds from raw materials such as plants, seeds, and biomass. It is frequently aided with *n*-hexane as a co-solvent. This binary system's variable solvating power minimizes the extraction of undesirable components while enabling the selective extraction of target compounds.[18] In the production of food and beverages, CO_2 and *n*-hexane binary systems are used for decaffeination, flavors, and fragrance extraction, and the elimination of unwanted substances including pesticides and pollutants. When needed, *n*-hexane can help with CO_2 extraction, which is a safe and effective way to extract high-quality food ingredients without sacrificing the integrity of the final product or leaving behind leftover solvents.[19,20] CO_2 and *n*-hexane binary systems are used as reaction media or solvents in a variety of synthesis processes in the chemical and pharmaceutical sectors. A green and adaptable solvent solution for catalytic reactions, polymerizations, and particle formation processes is provided by supercritical CO_2, which is frequently mixed with *n*-hexane. This binary system's special solvation characteristics allow for

exact control over reaction parameters, product selectivity, and particle shape, which improves both process effectiveness and product quality.[21,22]

The phase behavior (vapor–liquid equilibrium, VLE) of the carbon dioxide + *n*-hexane binary system was investigated in many papers, as can be seen in **Table 1**. It can be remarked that this system is often used as a model for validating new installations, and from the multitude of data reported at 313 K, seven isotherms belong to the same group.[23-27] Also, many authors report only the composition of the liquid phase (*x*) and the VLE data (*p*-*x*, *y*) reported by refs.[28, 29] are identical, except for temperatures (313 vs 313.15 K). Both references are in Chinese and we accessed the data reported by Yu et al.[29] via DETHERM database.[30] In **Table 1** are not mentioned the data measured by Han et al.[31], which are presented only graphically, those reported by King and Al-Najjar[32] at atmospheric pressure, and the isopleths measured by Choi et al.[33]

The critical behavior of the carbon dioxide + *n*-hexane system was also investigated by several groups, some of which are the critical points corresponding to the isotherms or isopleths measured[28, 29, 33], some are dedicated to the measurement of critical liquid–vapor line.[34,35,36,37,38] It is worth noting that the critical composition is reported only by Liu et al.[38] and Gurdial et al.[37] in the critical behavior dedicated studies, while the data presented in "Table I" by Leder and Irani[36] for "CO_2 + n-hexane" are in fact for CO_2 + cyclohexane, and the correct data are labelled as "CO_2 + hexane" in the same table. Also, the critical data presented in "**Table 1**" by Sun et al.[39] are in fact the citation of those published by Zhu et al.[28], and they are the same in the paper authored by Yu et al.[29]

An important study from 1971 is presented by Im and Kurata[40] who established that the carbon dioxide + *n*-hexane system belongs to what was defined later as type II phase behavior by van Konynenburg and Scott,[41] which encompasses two critical curves, one liquid–vapor (LV) joining the critical points of the pure components, the other one liquid–liquid (LL) which crosses with the equilibrium line of the three liquid–liquid–vapor (LLV) phases in an upper critical endpoint (UCEP). They measured the solid–liquid–vapor equilibrium curve up to an eutectic point of 176.7 K and estimated the temperature of the UCEP to be 213.7 K.[40]

We analyzed all available literature data, and we noticed that there is a high degree of scattering, sometimes even for measurements reported by the same group. One example is provided in **Figure 1**, where we compare all isotherms measured at about 313 K, and the liquid phase compositions

are really spread, but the observation is valid for most temperatures. Although the figure is very loaded, it can be easily observed that the difference in the composition of the liquid phase at the same pressure is sometimes greater than 0.4. We compared all VLE literature data in **Figures 1S.-9S.** (Supporting information – SI), in which we grouped the experimental data based on the number of sets measured at a given temperature (238 – 278 K, 283 – 293 K, 298 K, 303 K, 308 K, 318 – 328 K, 333 K, 353 K, 373 – 393 K). Overall, it seems that the highest differences can be observed in the liquid compositions at 273 K (**Figure 1S**: the data from ref.[42] are not in agreement with those of ref.[43], which seem more reliable based on the comparison at all temperatures), 283 K (**Figure 2S**: the data comes from the same research groups as for the previous temperature and the same observation applies), 298 K (**Figure 3S**: the data from refs.[42, 44] do not agree with the other ones), 313 K (**Figure 1**, the data from refs.[28, 29] are identical and very far from all other data, while the data reported by refs. [44-47] seem to not agree with those reported by the other research groups), 323 K (**Figure 6S**: the data from refs.[45, 48] are not in agreement with the other ones), 333 K (**Figure 7S**: the data from Zhu et al.[28] and Yu et al.[29] are identical and the difference in the liquid phase composition is higher than 0.4 at the same pressure compared with the other measurements at the same temperature; the data from Liu et al.[45] and Yang et al.[48] seem to agree each other, but they disagree with those reported by Leal et al.[47]), 353 K (**Figure 8S**: the same comment as for the previous temperature applies for the data from refs.[28, 29], while the data from Leal et al.[47] and Gui et al.[46] seem to be slightly off), and 373 K (**Figure 9S**: data from the same groups as for the previous temperature do not agree with those of Li et al.[49]). In summary, if we compare the VLE data all together, some isotherms deviate severely compared to most of the others (i.e., Zhu et al.[28] and Yu et al.[29], Gainar[42]), while other show smaller deviations (Ohgaki and Katayama[44], Gui et al.[46], Leal et al.[47], Koller et al.[15], and Liu et al.[45]). However, it is difficult to decide whether the purity of substances or the experimental errors could cause such differences. Moreover, some authors do not report the purity of substances used (e.g., Zhu et al.[28]).

Regarding the liquid–vapor critical available data, the same spread can be observed among diverse research groups, which could be explained by different methods used.

In this context, we report eight new isotherms ranging from 313.15 K to 383.15 K and the critical compositions, pressures, and temperatures up to the critical pressure maximum (CPM) of the liquid–vapor critical curve.

Table 1. Literature phase behavior for CO_2 (1) + *n*-hexane (2) binary system

T/K	p_{range}/bar	Nexp	Type	Method[a]	Reference
238.15	2.0265 ÷ 10.132	9	*p* – *x*	N.A.[a]	Shenderei & Ivanovskii, 1964[50]
273.15	10.66 ÷ 31.52	6	*p* – *x*	SynTX	Kaminishi et al., 1987[43]
273.16	5.68 ÷ 37.43	8	*p* – *x*	AnTCapX	Gainar, 2003[42]
278.16	8.13 ÷ 44.0	5	*p* – *x*	AnTCapX	Gainar, 2003[42]
283.15	12.41 ÷ 40.05	6	*p* – *x*	SynTX	Kaminishi et al., 1987[43]
283.16	12.54 ÷ 41.45	5	*p* – *x*	AnTCapX	Gainar, 2003[42]
288.16	9.99 ÷ 44.78	6	*p* – *x*	AnTCapX	Gainar, 2003[42]
293.15	17.0 ÷ 52.7	8	*p* – *x*	AnTVisVarX	Nemati Lay et al., 2006[51]
293.15	32.8 ÷ 50.7	5	*p* – *x*	SynVisX	Nemati Lay, 2010[52]
298.15	4.437 ÷ 52.057	10	*p* – *x*, *y*	AnTBlo	Ohgaki & Katayama, 1976[44]
298.15	15.28 ÷ 55.37	6	*p* – *x*	SynTX	Kaminishi et al., 1987[43]
298.15	17.0 ÷ 57.8	9	*p* – *x*	AnTVisVarX	Nemati Lay et al., 2006[51]
298.15	35.1 ÷ 55.5	5	*p* – *x*	SynVisX	Nemati Lay, 2010[52]
298.15	9.5 ÷ 46.8	10	*p* – *x*	SynVisVarX	Gao et al., 2021[53]
298.16	7.05 ÷ 52.33	9	*p* – *x*	AnTCapX	Gainar, 2003[42]
303.09	22.01 ÷ 69.82	11	*p* – *x*, *y*	AnTCapValVis	Williams-Wynn et al., 2016[27]
303.15	20.24 ÷ 67.46	7	*p* – *x*, *y*	AnTCap	Wagner & Wichterle, 1987[54]
303.15	19.3531 ÷ 67.1785	8	*p* – *x*, *y*	N.A.[a]	Chen & Chen, 1992[55]
303.15	16.19 ÷ 61.09	6	*p* – *x*	SynTX	Kaminishi et al., 1987[43]
303.15	38.3 ÷ 61.5	5	*p* – *x*	SynVisX	Nemati Lay, 2010[52]
303.15	0.249 ÷ 50.112	5	*p* – *x*	SynTVisX	Koller et al., 2019[15]
303.17	24.11 ÷ 61.64	4	*p* – *x*	SynVisVarX	Williams-Wynn et al., 2016[27]
308.15	62.9	1	*p* – *x*	N.A.[a]	Tolley, 1990[56]
308.15	17.0 ÷ 73.1	12	*p* – *x*	AnTVisVarX	Nemati Lay et al., 2006[51]
308.15	40.6 ÷ 66.5	5	*p* – *x*	SynVisX	Nemati Lay, 2010[52]
308.15	34.7 ÷ 68.0	5	*p* – *x*	AnTVisVarX	Yang et al., 2012[48]
313.00	21.5 ÷ 75	7	*p* – *x*, *y*	N.A.[b]	Zhu et al., 2006[28]
313.12	11.0 ÷ 76.94	12	*p* – *x*, *y*	AnTCapValVis	Williams-Wynn et al., 2016[27]
313.15	6.3196 ÷ 76.574	10	*p* – *x*, *y*	AnTBlo	Ohgaki & Katayama, 1976[44]
313.15	7.79 ÷ 74.81	10	*p* – *x*, *y*	AnTVal	Li et al., 1981[49]
313.15	20.84 ÷ 78.66	10	*p* – *x*, *y*	AnTCap	Wagner & Wichterle, 1987[54]
313.15	62.9 ÷ 75.0	2	*p* – *x*	N.A.[a]	Tolley, 1990[56]
313.15	21.50 ÷ 75.0	7	*p* – *x*,*y*	N.A.[a]	Yu et al., 2006[29]
313.15	43.5 ÷ 73.1	5	*p* – *x*	SynVisX	Nemati Lay, 2010[52]
313.15	27.1 ÷ 75.7	8	*p* – *x*, *y*	AnTLcirVcirValChro	Liu et al., 2022[45]
313.15	0.375 ÷ 80.21	14	*p* – *x*, *y*	AnTCapValVis	Nelson et al., 2021[23]
313.15	9.3 ÷ 68.3	10	*p* – *x*, *y*	AnTLcirVcirValChro	Gui et al., 2017[46]
313.15	28.1 ÷ 72.5	9	*p* – *x*	AnTCapValVisVarX	Nelson & Ramjugernath, 2017[26]
313.15	9.25 ÷ 77.72	8	*p* – *x*, *y*	AnTCapValVisVarX	Hassanalizadeh et al., 2019[24]
313.17	30.0 ÷ 66.3	5	*p* – *x*	SynVisX	Hassanalizadeh et al., 2019[24]
313.20	17.1 ÷ 63.0	4	*p* – *x*	SynVisX	Leal et al., 2018[47]
313.21	26.5 ÷ 73.65	4	*p* – *x*	SynVisVarX	Williams-Wynn et al., 2016[27]
313.21	3.45 ÷ 28.02	19	*p* – *x*	SynVisX	Ebrahiminejadhasanabadi et al., 2018[25]
313.50	20.3663 ÷ 78.2229	8	*p* – *x*, *y*	N.A.[a]	Chen & Chen, 1992[55]
318.15	36.2 ÷ 73.2	5	*p* – *x*	AnTVisVarX	Yang et al., 2012[48]
318.15	80.5	1	*p* – *y*	SynVisVar	Wang et al., 2005[57]
318.15	81.1 ÷82.5	2	*p* – *x*	SynVisVar	Wang et al., 2005[57]

Table 1. Literature phase behavior for CO_2 (1) + *n*-hexane (2) binary system (continued)

323.05	14.05 ÷ 83.34	10	*p* – *x*, *y*	AnTCapValVis	Williams-Wynn et al., 2016[27]
323.15	18.64 ÷ 84.94	9	*p* – *x*, *y*	AnTCap	Wagner & Wichterle, 1987[54]
323.15	18.2385 ÷ 84.6064	9	*p* – *x*, *y*	N.A.[a]	Chen & Chen, 1992[55]
323.15	72.2 ÷ 86.3	5	*p* – *y*	SynVisVarY	Wang et al., 2006[58]
323.15	37.4 ÷ 80.0	6	*p* – *x*	AnTVisVarX	Yang et al., 2012[48]
323.15	25.2 ÷ 83.7	8	*p* – *x*, *y*	AnTLcirVcirValChro	Liu et al., 2022[45]
323.23	29.13 ÷ 86.17	4	*p* – *x*	SynVisVarX	Williams-Wynn et al., 2016[27]
328.00	73.1 ÷ 89.3	5	*p* – *y*	SynVisY	Shi et al., 2015[59]
328.15	72.2 ÷ 89.5	5	*p* – *y*	SynVisVarY	Wang et al., 2006[58]
333.00	21.5 ÷88.7	7	*p* – *x*, *y*	N.A.[b]	Zhu et al., 2006[28]
333.15	21.5 ÷88.7	7	*p* – *x*,*y*	N.A.[a]	Yu et al., 2006[29]
333.15	80.8 ÷ 92.5	4	*p* – *y*	SynVisVarY	Wang et al., 2006[58]
333.15	38.0 ÷ 86.7	6	*p* – *x*	AnTVisVarX	Yang et al., 2012[48]
333.15	23.9 ÷ 94.0	8	*p* – *x*, *y*	AnTLcirVcirValChro	Liu et al., 2022[45]
333.20	21.2 ÷ 84.9	4	*p* – *x*	SynVisX	Leal et al., 2018[47]
343.15	29.7 ÷ 110.3	8	*p* – *x*, *y*	AnTLcirVcirValChro	Liu et al., 2022[45]
353.00	31.6 ÷110.0	8	*p* – *x*, *y*	N.A.[b]	Zhu et al., 2006[28]
353.15	31.6 ÷110.0	8	*p* – *x*, *y*	N.A.[a]	Yu et al., 2006[29]
353.15	8.62 ÷ 106.59	14	*p* – *x*, *y*	AnTVal	Li et al., 1981[49]
353.15	16.5 ÷ 98.7	9	*p* – *x*	SynVisVarX	Gao et al., 2021[53]
353.15	15.6 ÷ 105.8	11	*p* – *x*, *y*	AnTLcirVcirValChro	Gui et al., 2017[46]
353.20	25.5 ÷ 105.4	4	*p* – *x*	SynVisX	Leal et al., 2018[47]
373.00	42.1 ÷126.3	5	*p* – *x*, *y*	N.A.[b]	Zhu et al., 2006[28]
373.15	42.1 ÷126.3	6	*p* – *x*, *y*	N.A.[a]	Yu et al., 2006[29]
373.20	29.8 ÷ 113.1	4	*p* – *x*	SynVisX	Leal et al., 2018[47]
393.15	8.96 ÷ 115.97	15	*p* – *x*, *y*	AnTVal	Li et al., 1981[49]
393.20	34.0 ÷ 103.1	3	*p* – *x*	SynVisX	Leal et al., 2018[47]
393.20	114.5	1	*p* – *y*	SynVisY	Leal et al., 2018[47]

N.A. – Not available; [a]Experimental data collected from Detherm database[30]; [b]in Chinese.

The new and literature data were also modeled. Firstly, we correlated all the vapor–liquid equilibrium – VLE experimental data for the carbon dioxide + *n*-hexane system with the models **G**eneral **E**quation **O**f **S**tate – GEOS,[60,61,62] Peng–Robinson – PR[63], and Soave–Redlich–Kwong – SRK[64] in association with classical van der Waals mixing rules, i.e., one- and two-parameter conventional combining rules (1PCMR and 2PCMR). We also used PPR78[65,66,67,68] model. The influence of pure components parameters (critical data and acentric factor) from various database (DIPPR,[69] Poling et al., 2000,[70] Reid et al., 1987[71]) was checked as well. We then modeled the system, including the critical curves, with unique sets of binary interaction parameters for each equation of state that we obtained through a strategy similar to the one we used recently.[72,73] Furthermore, we compared different binary systems containing carbon dioxide and C6 compounds

(*n*-alkane, cycloalkane, branched alkane), as they could be used in carbon capture and storage (CCS) applications.[74,75]

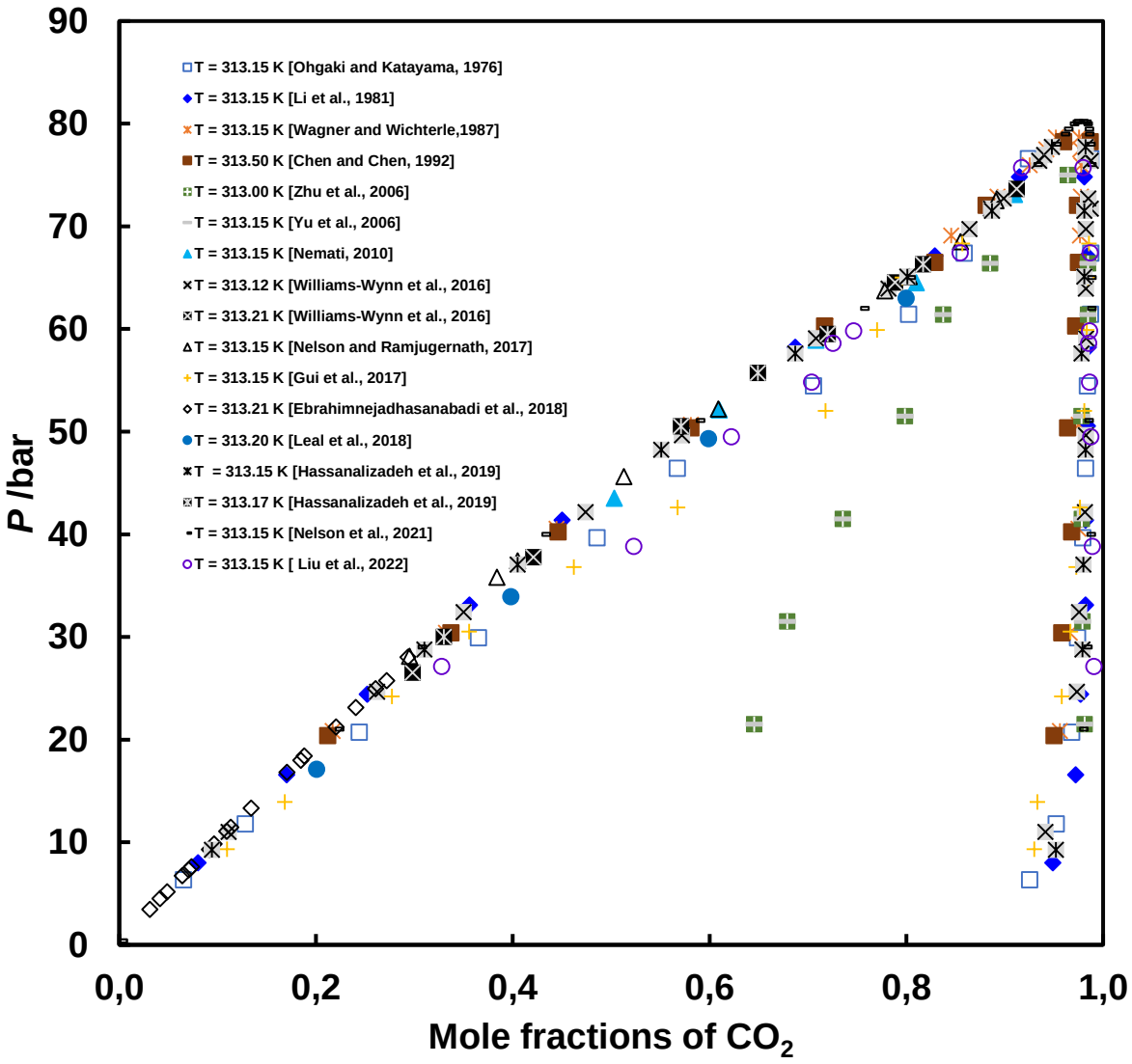

Figure 1. Comparison of literature vapor–liquid equilibrium data at 313 K.

2. EXPERIMENTAL SECTION

2.1. Materials

Both CO_2 and *n*-hexane used in the experimental determinations (VLE, and critical LV curve) were of very high purity and therefore employed without supplementary purification. However, the purities reported by the manufacturers (**Table 2**) were confirmed by GC analysis for both components.

Table 2. Purities and manufacturers of substances used in this work.

Compound	Purity	Manufacturer
Carbon dioxide	Min. 99.9995% (mole fraction)	Linde
n-Hexane	ReagentPlus®, ≥99% (mass fraction)	Sigma-Aldrich

2.2. Apparatus and Procedure

The carbon dioxide + *n*-hexane binary system was examined in the same high-pressure installation as described precisely in our previous publications,[73, 76] utilizing identical procedures for VLE and critical curve measurements. In brief, the setup includes a 60 cm^3 stainless steel visual cell with two sapphire windows, two ROLSI[77] valves, a gas chromatograph, a high-pressure Teledyne Isco syringe pump, vacuum pump, etc. The isotherms were recorded using the method named "*AnTVisVarCap*" by Dohrn and co-workers,[1,2,3,4,78,5,6] while the critical curve measurement procedure used is denoted by the same authors as "*AnTVisVarCapPcTc*". The uncertainties of the platinum probe and of pressure are assessed to be within ± 0.1 K and ± 0.015 MPa for a pressure span between (0.5 and 20) MPa respectively.

3. RESULTS AND DISCUSSION

3.1. Experimental Data

Pressure-phase compositions (liquid and vapor) data measured at eight constant temperatures (313.15, 323.15, 333.15. 343.15, 353.15, 363.15, 373.15, and 383.15 K) and pressures up to 117 bar are given in **Table 3**, while the new experimental critical curve is provided in **Table 4**, both together with their standard uncertainties. The new isothermal data are depicted in **Figure 2** and compared with corresponding literature data in **Figures 3-8** and, generally, the new data are in good agreement with those data that are already in good correspondence, as we explained in the Introduction (i.e., except for the data published by refs.[45, 47]). Two isotherms (363.15 and 383.15 K) are for the first time measured.

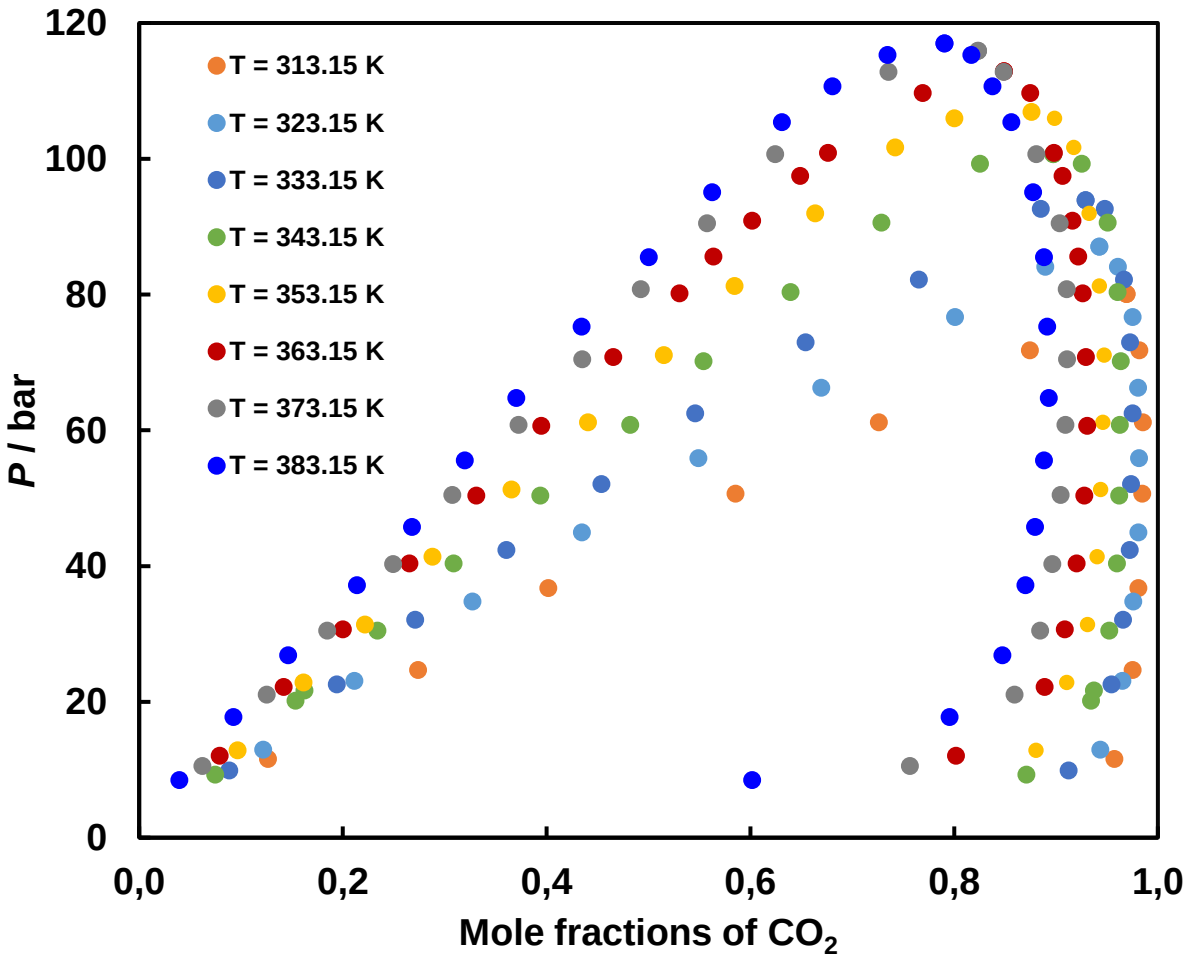

Figure 2. Isothermal VLE data measured at eight temperatures.

Table 3. Mole fractions of component 1 in the liquid (x_1) and vapor (y_1) phases, at various temperatures (T), and pressures (P), for the binary system carbon dioxide (1) + *n*-hexane (2).

P/bar	x_1	y_1	P/bar	x_1	y_1
		T/K = 313.15 ± 0.1			
11.6	0.1263	0.9571	61.2	0.7261	0.9852
24.7	0.2738	0.9751	71.8	0.8742	0.9818
36.8	0.4016	0.9809	80.1	0.9691	0.9691
50.7	0.5852	0.9845			
		T/K = 323.15 ± 0.1			
13.0	0.1217	0.9435	66.3	0.6695	0.9803
23.1	0.2112	0.9651	76.7	0.8008	0.9751
34.8	0.3270	0.9756	84.1	0.8895	0.9608
45.0	0.4345	0.9808	87.1	0.9424	0.9424
55.9	0.5487	0.9813			
		T/K = 333.15 ± 0.1			
9.9	0.0884	0.9124	62.5	0.5456	0.9751
22.6	0.1939	0.9544	73.0	0.6541	0.9726
32.1	0.2709	0.9658	82.2	0.7653	0.9667
42.4	0.3605	0.9724	92.7	0.8851	0.9479
52.1	0.4538	0.9736	93.9	0.9218	0.9218
		T/K = 343.15 ± 0.1			
9.3	0.0744	0.8709	60.8	0.4819	0.9627
20.2	0.1533	0.9342	70.2	0.5538	0.9634
21.7	0.1623	0.9372	80.4	0.6393	0.9604
30.5	0.2337	0.9521	90.6	0.7285	0.9507
40.4	0.3086	0.9596	99.3	0.8254	0.9252
50.4	0.3937	0.9619	100.7	0.8972	0.8972
		T/K = 353.15 ± 0.1			
12.9	0.0964	0.8802	71.1	0.5148	0.9472
22.9	0.1613	0.9105	81.3	0.5842	0.9424
31.4	0.2215	0.9309	92.0	0.6635	0.9325
41.4	0.2879	0.9402	101.7	0.7420	0.9172
51.3	0.3655	0.9438	106.0	0.8003	0.8985
61.2	0.4404	0.9459	106.9	0.8760	0.8760
		T/K = 363.15 ± 0.1			
12.1	0.0789	0.8017	80.2	0.5304	0.9262
22.2	0.1416	0.8888	85.6	0.5636	0.9218
30.7	0.1997	0.9085	90.9	0.6017	0.9159
40.4	0.2652	0.9200	97.5	0.6486	0.9062
50.4	0.3309	0.9277	100.9	0.6761	0.8979
60.7	0.3946	0.9304	109.7	0.7692	0.8746
70.8	0.4652	0.9294	112.9	0.8489	0.8489
		T/K = 373.15 ± 0.1			
10.6	0.0621	0.7564	70.5	0.4349	0.9108
21.1	0.1252	0.8593	80.8	0.4922	0.9105
30.5	0.1843	0.8844	90.5	0.5574	0.9034

40.3	0.2493	0.8964	100.7	0.6243	0.8806
50.5	0.3073	0.9044	112.8	0.7353	0.8484
60.8	0.3722	0.9093	115.9	0.8234	0.8234
		T/K = 383.15 ± 0.1			
8.5	0.0394	0.6017	75.3	0.4343	0.8912
17.8	0.0925	0.7955	85.5	0.5000	0.8882
26.9	0.1462	0.8474	95.1	0.5625	0.8774
37.2	0.2136	0.8698	105.4	0.6308	0.8562
45.8	0.2678	0.8792	110.7	0.6804	0.8376
55.6	0.3196	0.8881	115.3	0.7345	0.8168
64.8	0.3702	0.8928	117.0	0.7904	0.7904

Standard uncertainties: $u(T)$ = 0.1 K, $u(p)$ = 0.1 bar, $u(x_1)$ = 0.001, $u(y_1)$ = 0.005.

Table 3. **Vapor-liquid critical curve for CO_2 (1) + *n*-hexane (2)**

***T*/K**	***P*/bar**	x_1	***T*/K**	***P*/bar**	x_1
304.21[a]	73.83[a]	1.0000	346.55	102.9	0.8892
312.85	79.6	0.9699	350.55	105.1	0.8818
313.15	80.1	0.9691	352.25	106.5	0.8766
316.65	82.3	0.9596	353.15	106.9	0.8760
322.65	86.8	0.9432	360.95	111.7	0.8548
323.15	87.1	0.9424	362.65	112.5	0.8496
326.75	89.8	0.9337	363.15	112.9	0.8489
333.15	93.9	0.9218	366.15	114.3	0.8393
336.05	95.9	0.9165	367.85	114.9	0.8347
342.75	100.5	0.8980	373.15	115.9	0.8234
343.15	100.7	0.8972	383.15	117.0	0.7904
344.85	101.7	0.8941	507.60[a]	30.25[a]	0.0000

Standard uncertainties: $u(T)$ = 0.5 K, $u(P)$ = 0.2 bar, $u(x_1)$ = 0.005; [a]DIPPR database values[69].

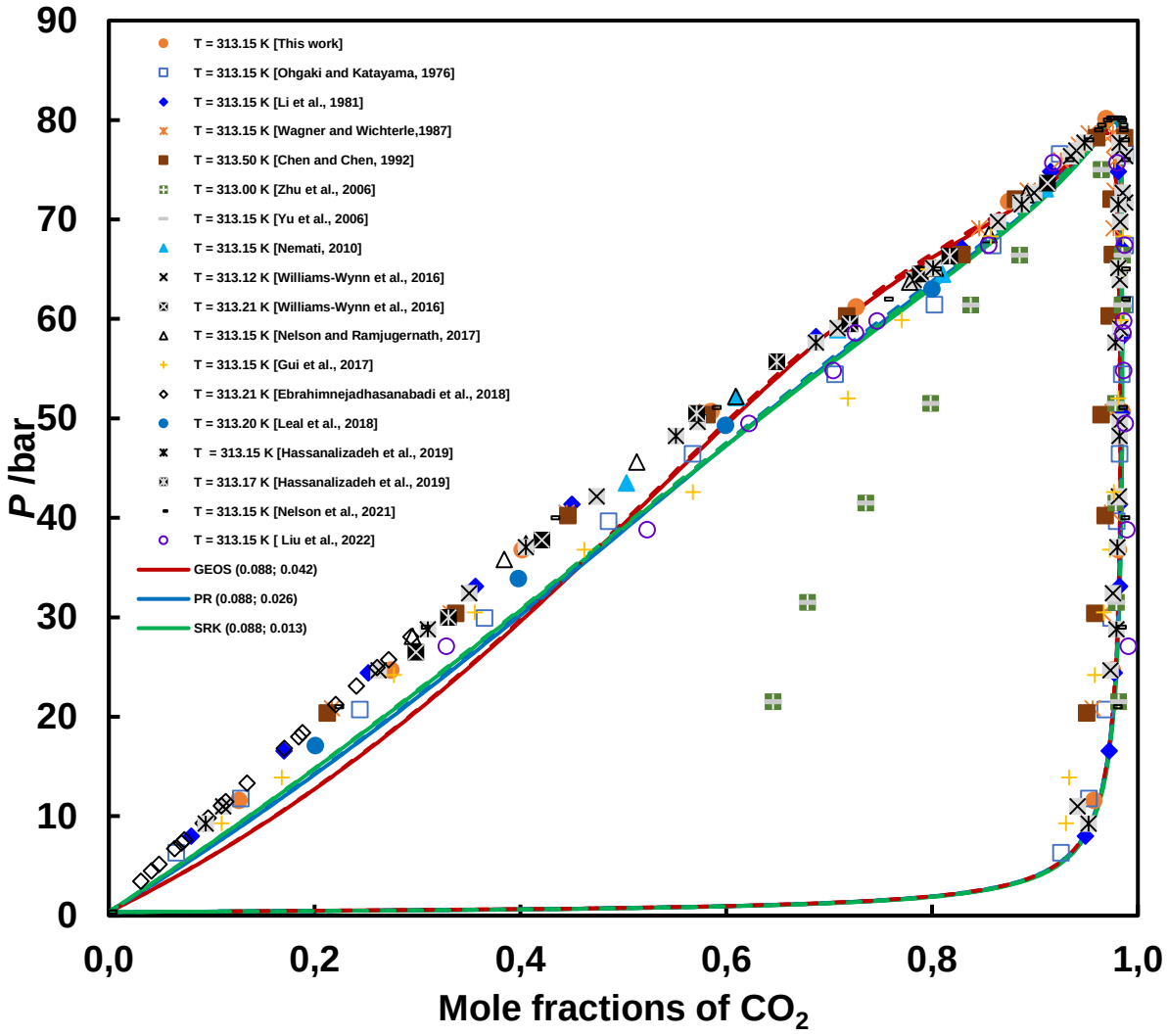

Figure 3. Comparison of new and literature VLE data at 313 K with model results.

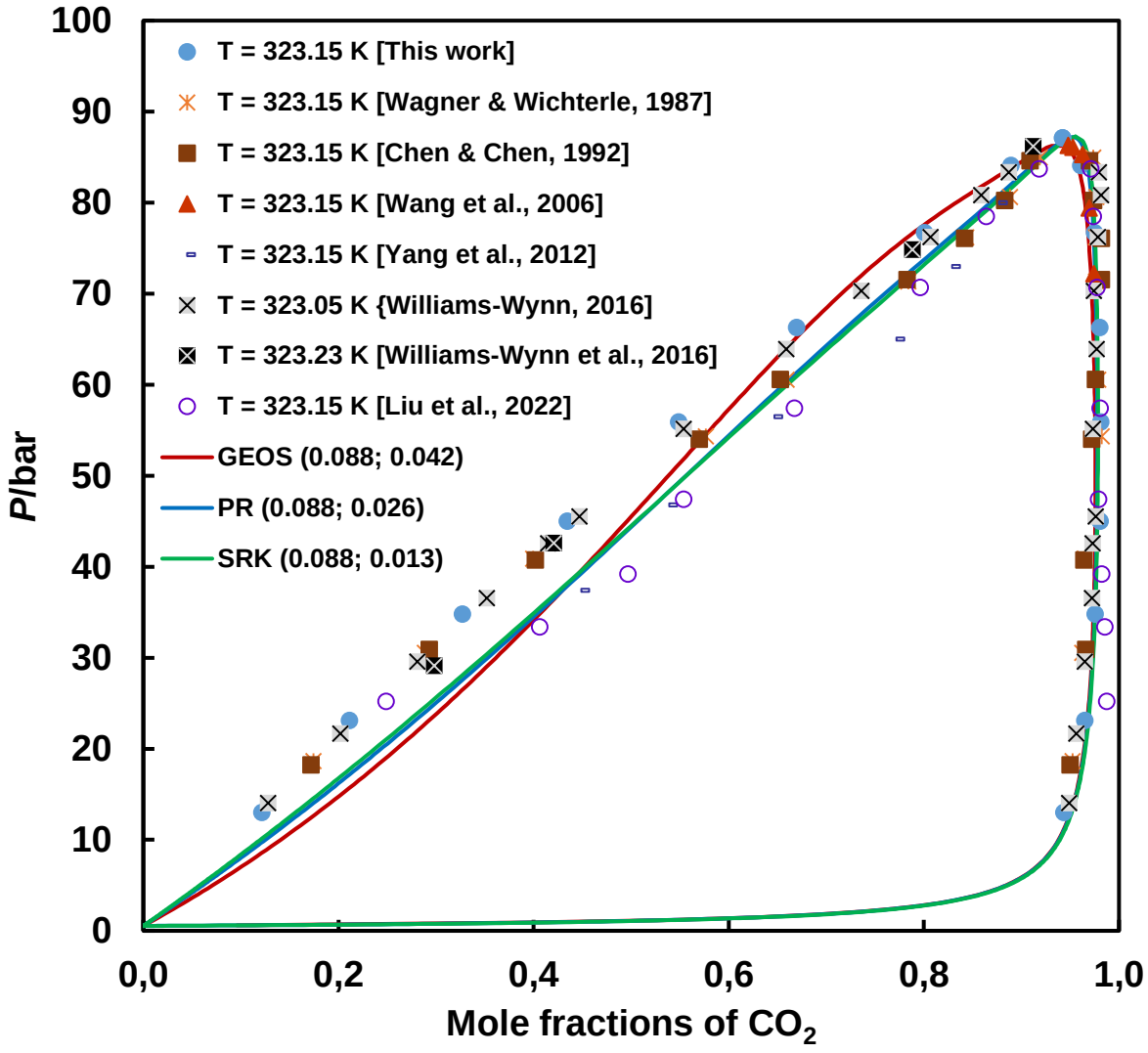

Figure 4. Comparison of new and literature VLE data at 323 K with model results.

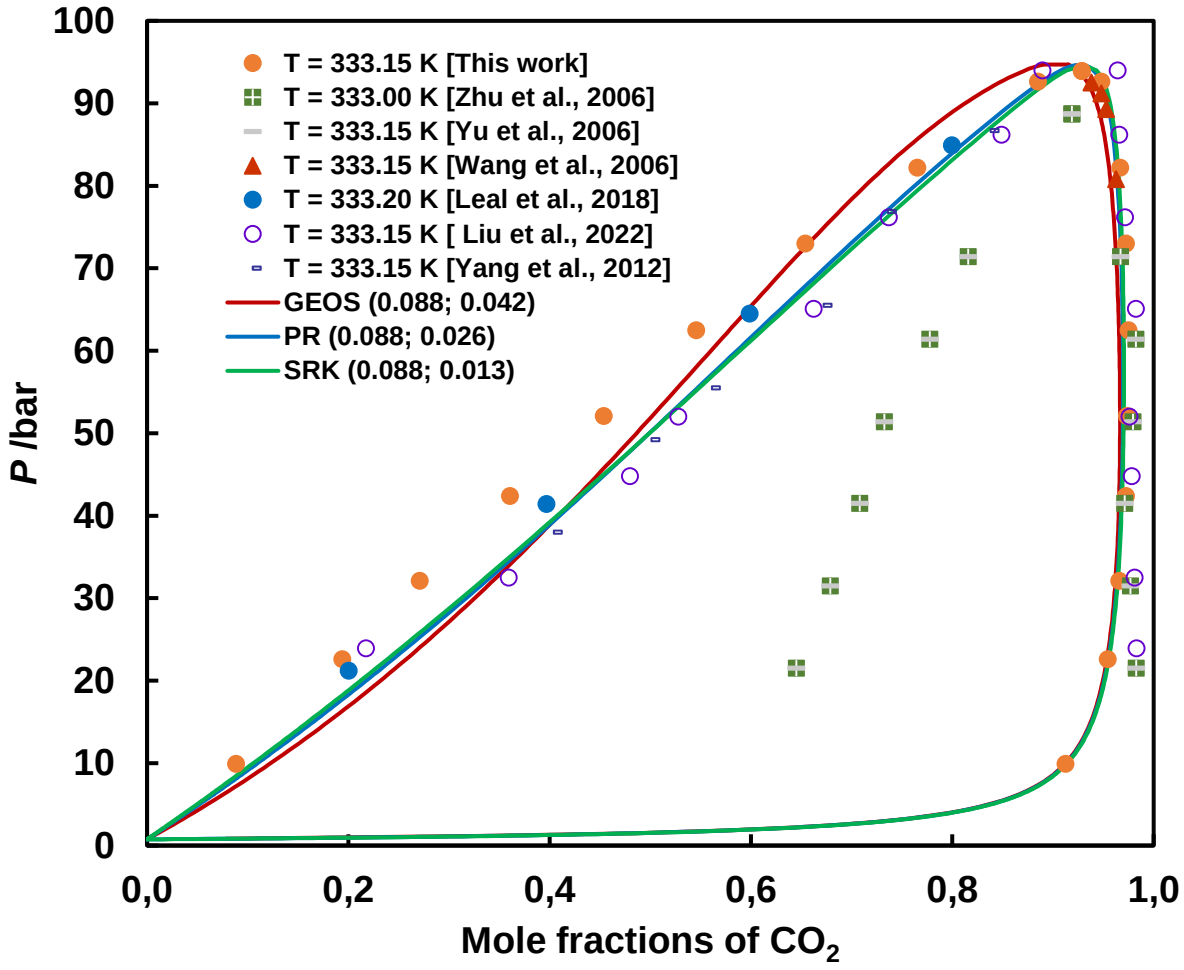

Figure 5. Comparison of new and literature VLE data at 333 K with model results.

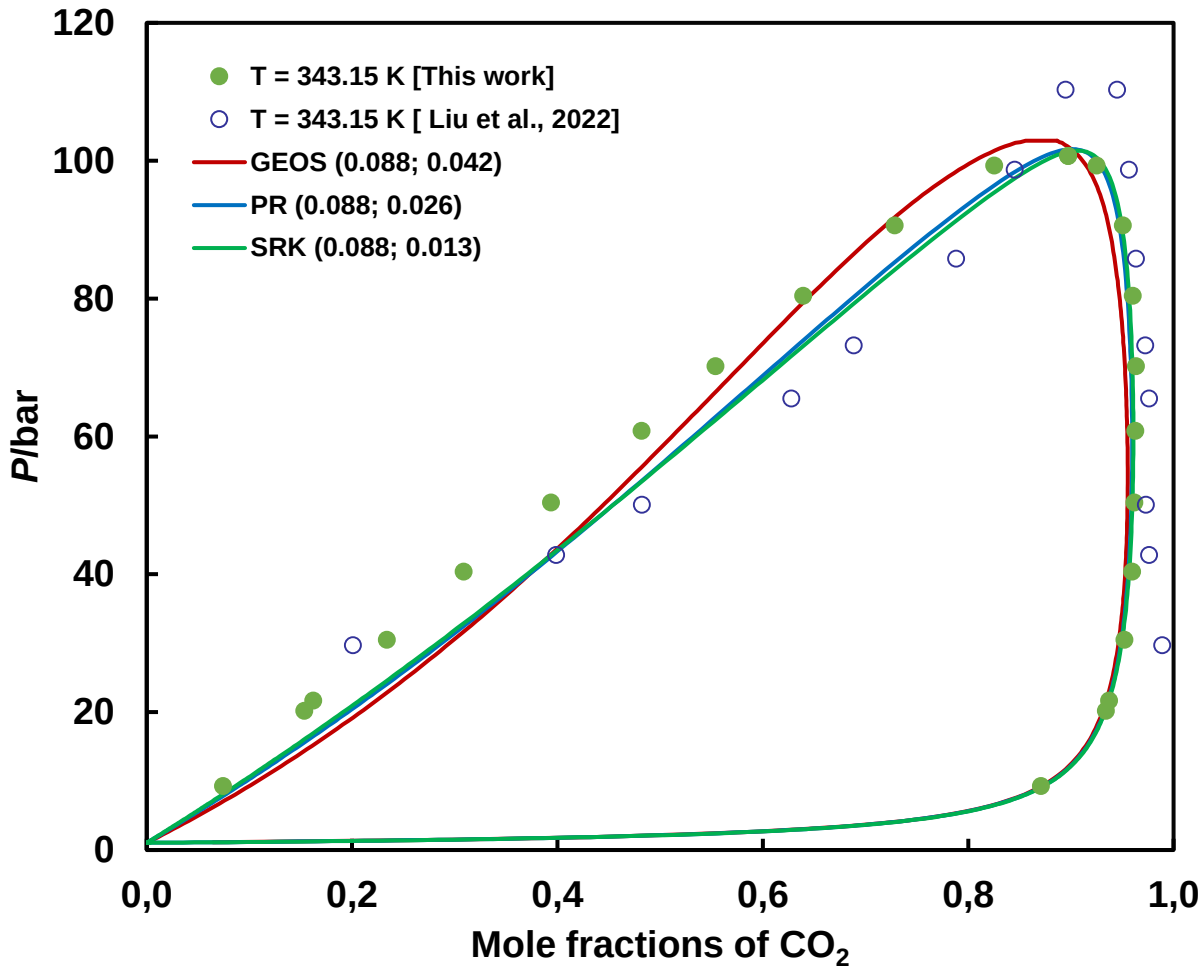

Figure 6. Comparison of new and literature VLE data at 343 K with model results.

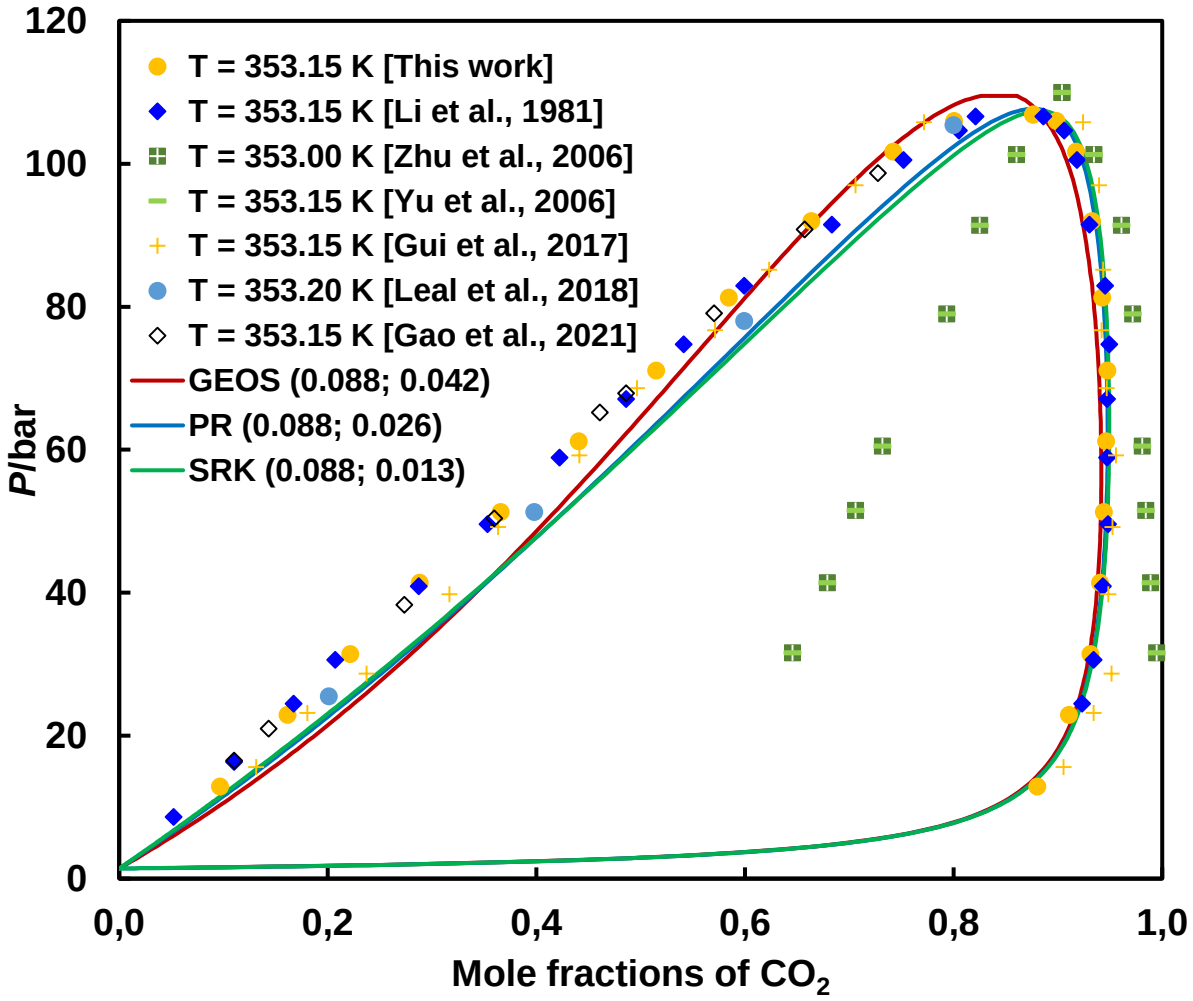

Figure 7. Comparison of new and literature VLE data at 353 K with model results.

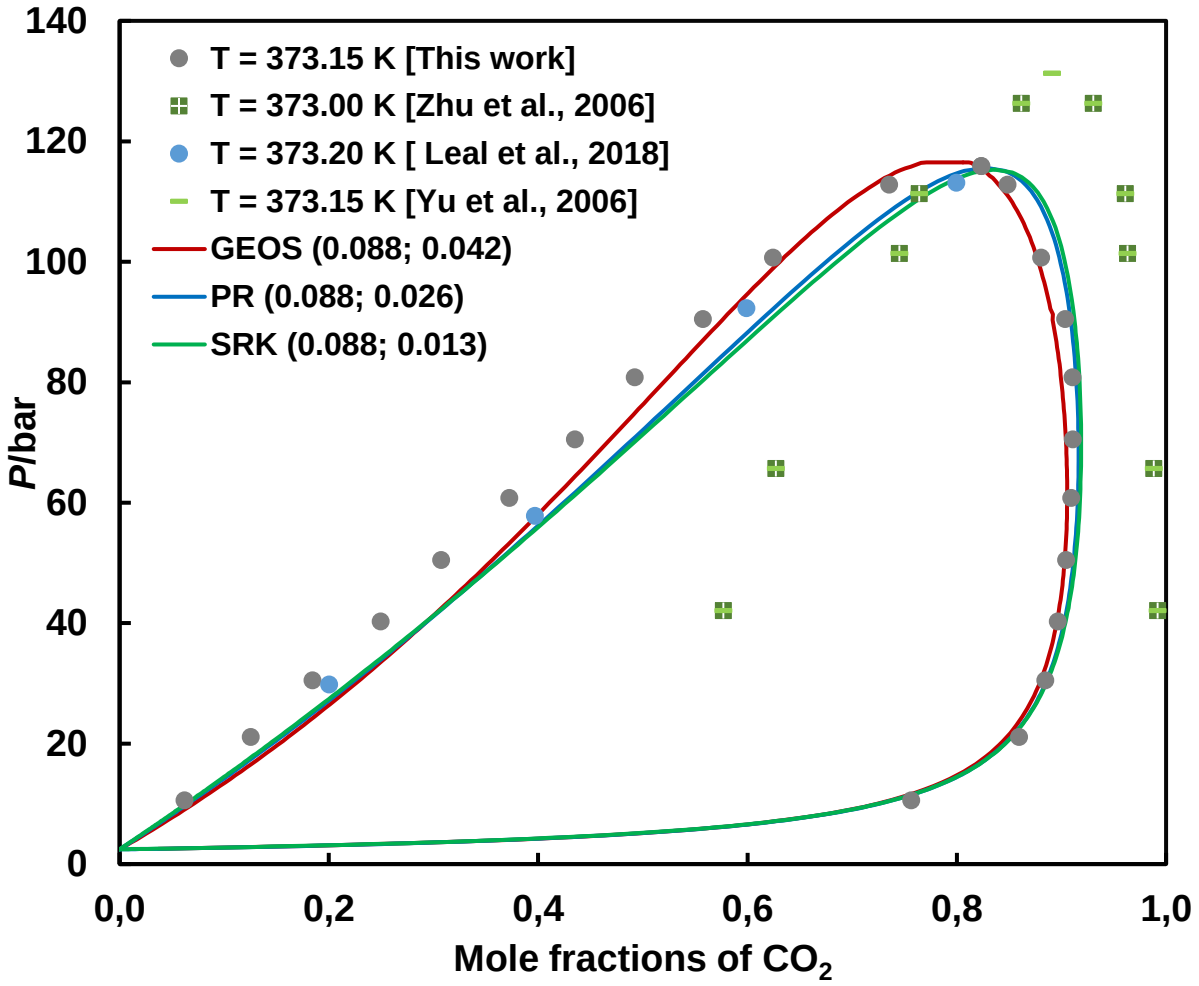

Figure 8. Comparison of new and literature VLE data at 373 K with model results.

3.2. Modeling

The new and literature data were firstly correlated with GEOS,[60-62] PR,[63] and SRK[64] thermodynamic models (equations provided in SI) with one- and two-conventional parameters combining rules. As expected, the correlations lead to small errors in calculated pressures, the values of average absolute deviations in pressure – AADP, % were less than 2% for most temperatures and for all three models which behave similarly. More specifically, the errors were higher for the data sets which were not in agreement with each other, as can be seen from **Figure 9**, where we illustrated the correlation results for two-parameter combining rules. The AADP, % is defined as:

$$AADP, \% = \frac{1}{N_{exp}} \cdot \sum_{i=1}^{N_{exp}} \left| \frac{p_i^{exp} - p_i^{calc}}{p_i^{calc}} \right| \cdot 100 \qquad (1)$$

where “exp” stands for experimental and “calc” for calculated.

The correlations by GEOS, PR, and SRK/2PCMR for the new isothermal experimental data are shown in **Figure 10S** and the calculations by all three models almost overlap. However, as temperature increases the critical point is slightly overestimated by PR and SRK and underestimated by GEOS. Consequently, the calculated vapor compositions present higher errors.

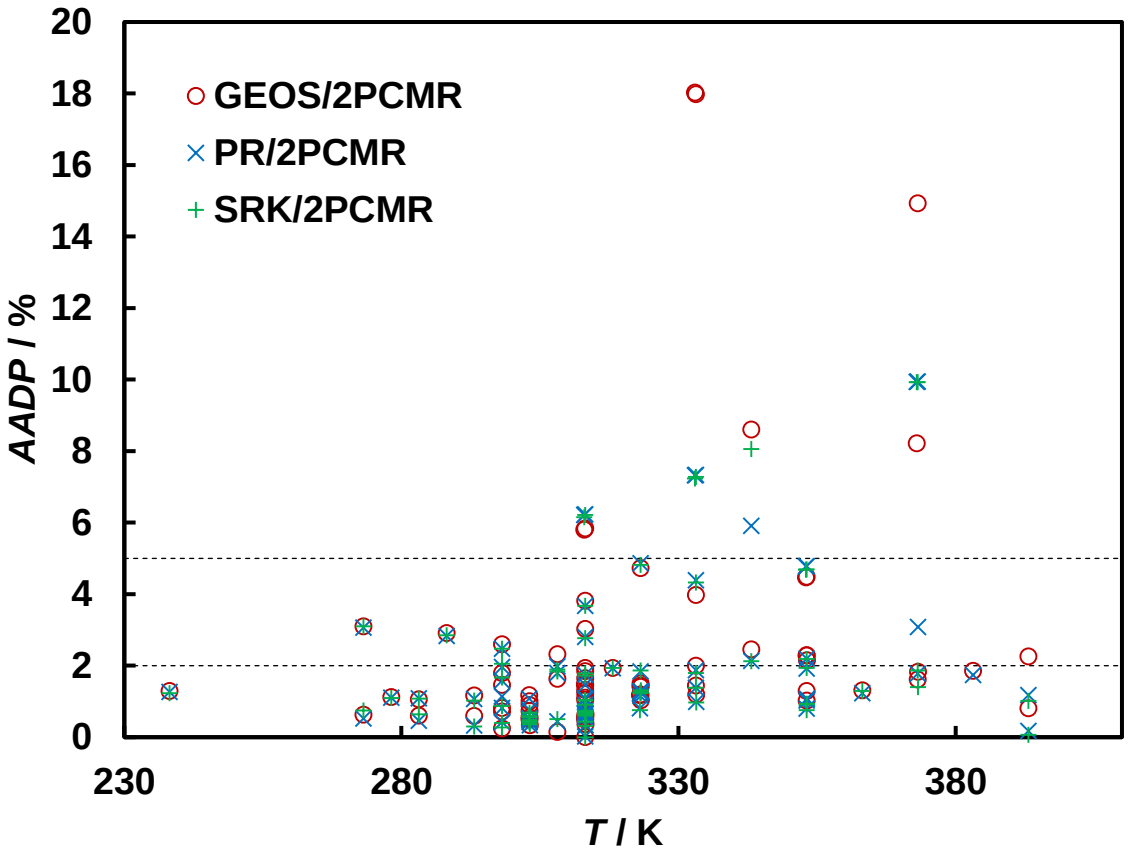

Figure 9. AADP, % as function of temperatures for correlation with GEOS, PR, and SRK/2PCMR.

Table 4. Pure component properties[69].

Substances	***Critical temperature*** T_c**/K**	***Critical pressure*** P_c**/bar**	***Critical volume*** V_c**/cm^3·mol^{-1}**	***Acentric factor*** ω
Carbon dioxide	304.21	73.83	93.90	0.223621
n-Hexane	507.60	30.25	371.00	0.301261
Cyclohexane	553.80	40.80	346.92	0.208050

In recent studies,[72,73,76,79,80,81,82] we examined the influence of critical data and acentric factors of pure components from various sources on the phase behavior calculation of the binary system and we concluded that they can contribute or not to better correlations, depending on the system. Moreover, we observed that other authors mix these data (e.g., Table 7 in ref[83]) to obtain better modeling results. Our calculations showed that for the carbon dioxide + *n*-hexane binary system, as for CO_2 + 2,4-dimethylpentane system,[76] there are not significant differences when using critical data and acentric factors for pure compounds from different database. Therefore, we show the results using the pure compounds critical data and acentric factors (**Table 4**) from DIPPR database,[69] as recommended by other authors.[68,84]

Recently,[72, 85] we showed that it is possible to model a binary system with good results using binary interaction parameters determined for another system. Thus, the binary interaction parameters (BIPs) determined by k_{12}-l_{12} method[75,86] for the carbon dioxide + 2-butanol binary system with the same three cubic equations of state were used to predict the phase behavior of various binary systems containing CO_2 and as second component substances with four carbon atoms (i.e., *n*-butane, 1-butanol, 1,2-dimethoxyethane, ethyl acetate, 1,4-dioxane). Therefore, the next step in our modeling strategy was to model the carbon dioxide + *n*-hexane system with the BIPs determined for the carbon dioxide + 1-hexanol system (k_{12} = 0.088; l_{12} = –0.033). However, the difference between the calculated critical pressure maximum and the experimental one ranged from about 4 to 14 bar, the smallest deviation being obtained with SRK model (**Figure 11S**). This behavior is not surprising as alcohols are self-associating compounds. Consequently, we customized these BIPs for each model in order to reproduce as best as possible the critical pressure maximum using a trial-and-error procedure. The new BIPs for each model are given in **Table 5**. While the first binary interaction parameter (k_{12}) is less sensitive, the second one (l_{12}) influenced the displacement of CPM. All three models predict type II phase behavior with the BIPs given in **Table 5**. The new experimental and literature critical data are compared with the results of the three models in **Figure 10**. Some disagreement between the experimental data from the literature can be noticed. We also added to the same figure the calculation results with the PPR78 model. It can be observed that PPR78 model behaves similarly to GEOS, PR, and SRK, and critical pressure maximum is less than 1 bar higher than the experimental one (117.0 bar) for all models. The difference between model results is the location of the corresponding critical temperature which is shifted to the right in the order PPR78<PR<SRK, while GEOS is almost the same with the

experimental one (383.15 K). The predicted critical pressures maximum and corresponding temperatures are also given in **Table 5**.

Table 5. Binary interaction parameters and the pressures and temperatures of CPM.

EoS/Mixing rule	k_{12}	l_{12}	CPM	
			T_c/K	P_c/bar
GEOS/2PCMR	0.088	0.042	383.00	117.49
PR/2PCMR	0.088	0.026	388.77	117.62
SRK/2PCMR	0.088	0.013	390.44	117.63
PPR78	f(T)	-	384.39	117.75

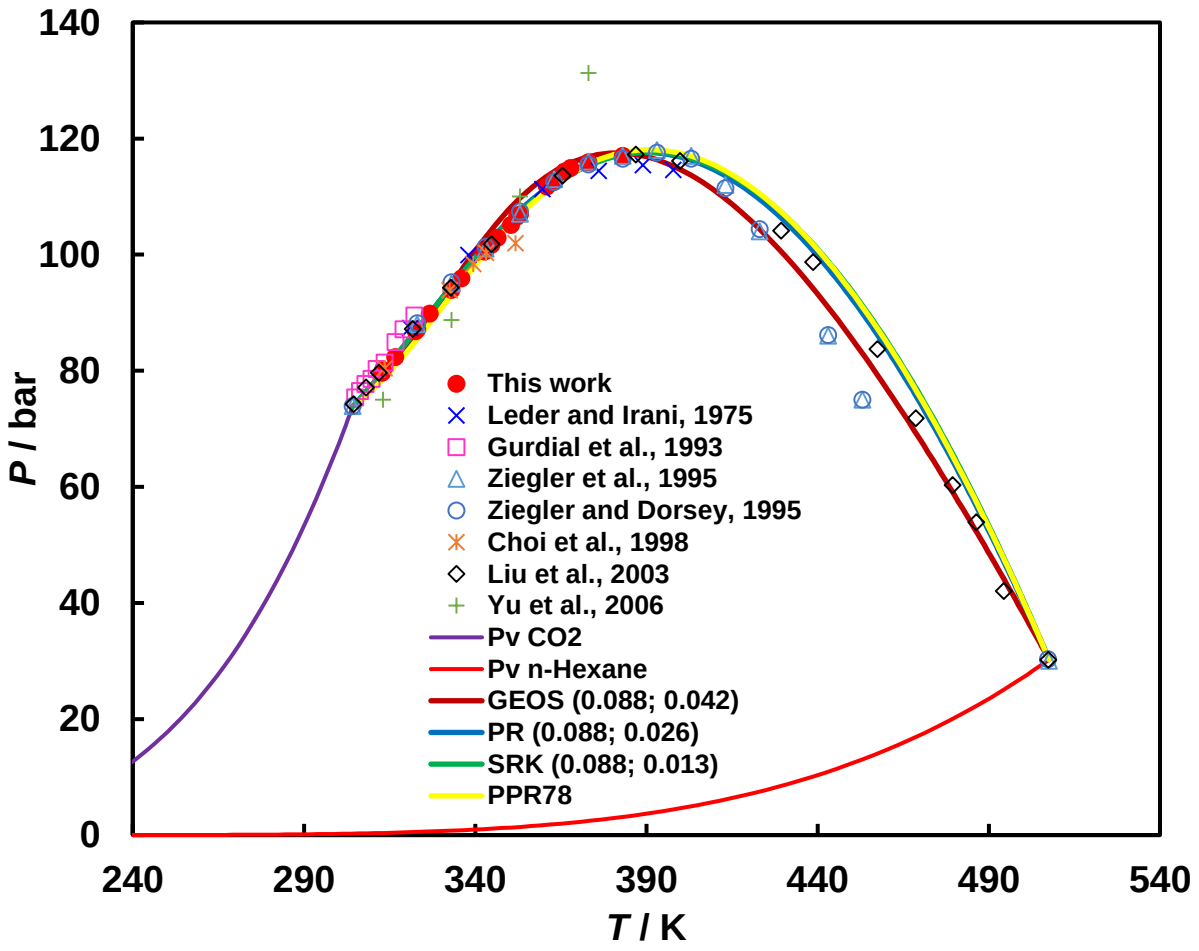

Figure 10. *P*–*T* fluid phase diagram of the carbon dioxide (1) + *n*-hexane (2) system.

Since neither the experimental liquid–liquid critical curve nor the equilibrium LLV line of the three phases are available, these curves were not drawn in **Figure 10** as predicted by the

thermodynamic models used (at very low temperatures, i.e., ~205 K). The pressure-composition and temperature-composition projections of the liquid–vapor curve are shown in **Figures 11** and **12**. The experimental literature compositions, as previously mentioned, are available only from Choi et al.[33] and Liu et al.[38] SRK and PR, followed by PPR78 and GEOS reproduce well the new critical data in both projections, as well as the data of Liu et al.[38] in the temperature-composition projection of the liquid–vapor critical curve. The calculation results by GEOS, PR, and SRK with the unique sets of BIPs from **Table 5** are shown in **Figures 3-8** and **12S-19S** respectively, covering both new and all literature data. Detailed comparisons of GEOS, PR, and SRK calculations with these sets of parameters, as well as correlations are presented for the new data in **Figures 20S-26S**.

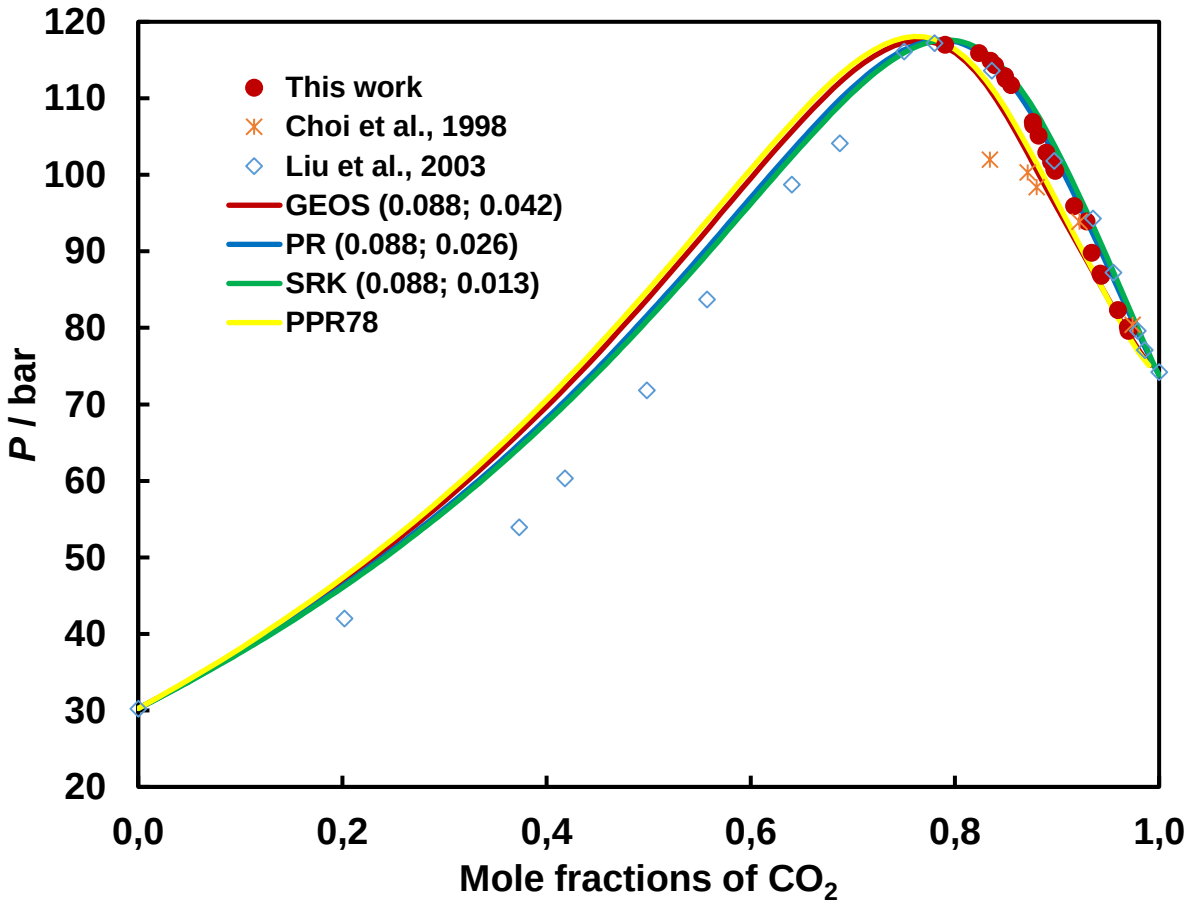

Figure 11. *P*– X_1 projection of the LV critical curve of the carbon dioxide (1) + *n*-hexane (2) system.

When we assess the three models (**Figures 20S-23S**) using the sets of BIPs given in **Table 5**, it can be seen that the differences are small and the experimental data are better predicted by GEOS, followed by PR and SRK. When we compare the correlation and prediction results with a single set of parameters (**Figures 24S-26S**), the variations between the models are also small, but GEOS reproduces the critical points better.

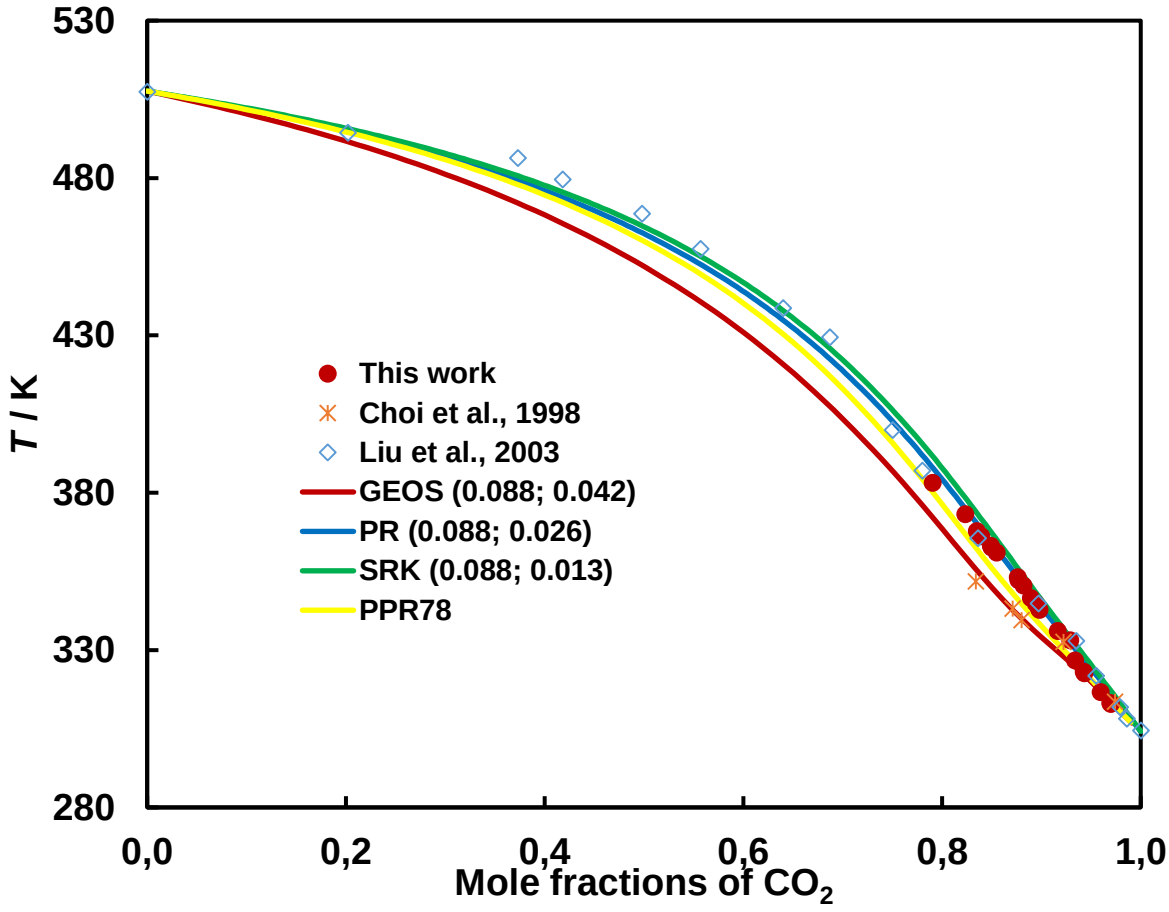

Figure 12. T– X_1 projection of the LV critical curve of the carbon dioxide (1) + *n*-hexane (2) system.

Finally, we compared the critical behavior of carbon dioxide + *n*-hexane and carbon dioxide + cyclohexane (CyC6), as both systems could be of interest for carbon capture and storage (CCS) applications.[53, 74, 75] As an example, we plotted in **Figure 13** all available experimental data for both systems together with the calculations with PR model only, to avoid loading the figure even more. Although the available experimental data for carbon dioxide + cyclohexane are in clear disagreement, the model (the upper green curve(s)) reproduces well the experimental critical

curve. Also, it can be noticed that the cycloalkane is more soluble than the *n*-alkane.[75] In regards to the model calculations, we used parameters determined for CO_2 + *n*-hexane (k_{12} = 0.086; l_{12} = 0.026) to calculate the critical behavior of the CO_2 + cyclohexane system, we also illustrated the results of PR modeling with parameters k_{12} = 0.1251 and l_{12} = -0.0276 determined specifically in another work[87] for CO_2 + cyclohexane, as well as with parameters k_{12} = 0.1162 and l_{12} = 0.0018 determined by Sima et al.[75] for CO_2 + *n*-hexane using a special objective function. The modeling results are very good for both systems when using parameters tuned for the other system and vice versa, indicating that for these types of systems preliminary modeling can be achieved if experimental data are not available.

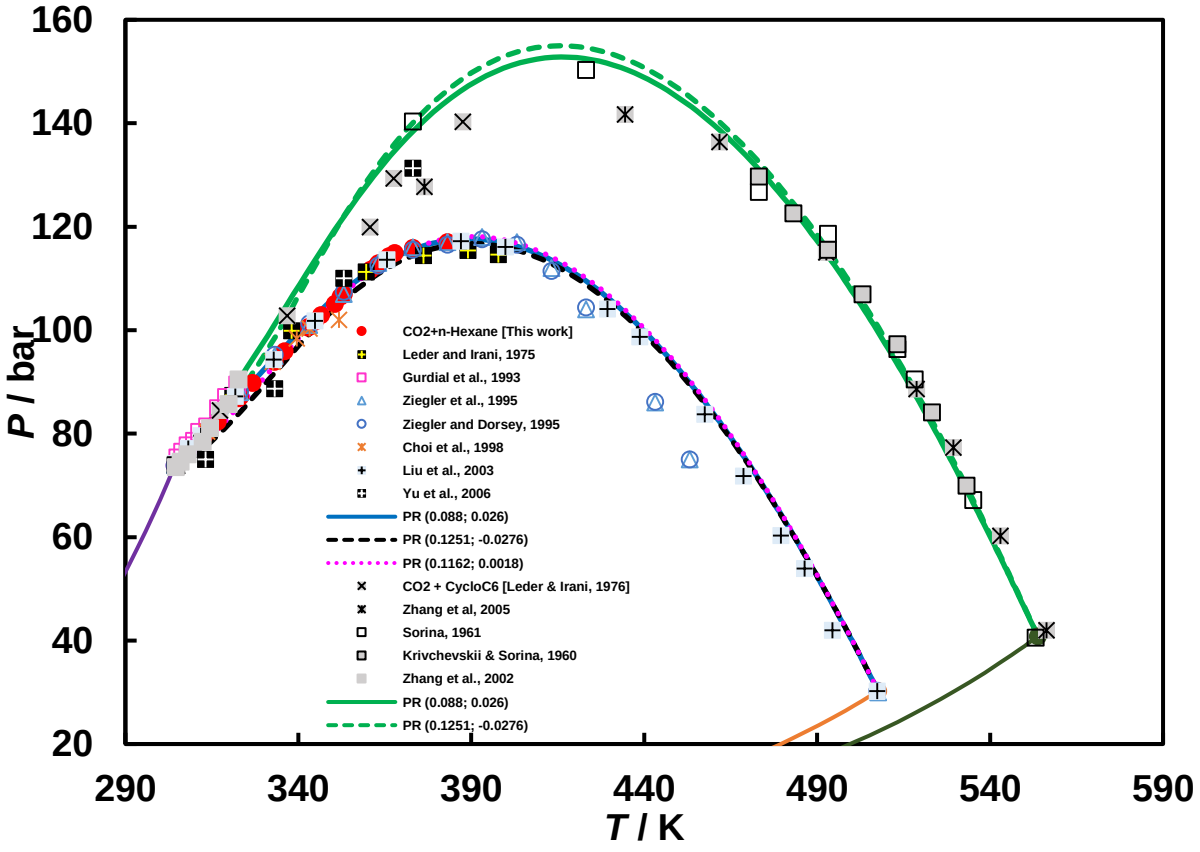

Figure 13. *P*–*T* fluid phase diagram of the carbon dioxide (1) + *n*-hexane (2) and carbon dioxide (1) + cyclohexane (2) systems. The experimental data for CO_2 + CyC6 are from Leder and Irani[36], Sorina[30], Krivchevskii and Sorina[30], Zhang et al., 2005[88], and Zhang et al., 2002.[30]

On the other hand, we tested the same sets of parameters for the carbon dioxide (1) + 2,3-dimethylbutane (2,3-DMB) – the position isomer for *n*-hexane, and in this case the results are not as good as for the cycloalkane, the difference in critical maximum pressure is –5 or –6 bar, compared to the experimental one.[89] A possible explanation is the structure of the branched alkane and the interactions it exhibits at high pressures with CO_2.

CONCLUSIONS

New vapor–liquid equilibrium data are reported at eight temperatures ranging from 313.15 K to 383.15 K as well as the liquid-vapor critical curve up to 117 bar and 383.15 K. The new data agree with the majority of already published ones. The available experimental literature data was reviewed and analyzed. Although apparently the availability of experimental data for this system is very good, it can be noticed a high degree of scatter. The system was successfully modeled with several thermodynamic models (GEOS, PR, SRK, and PPR78) using both correlations and a semi-predictive strategy. The critical data and acentric factors of pure components are similar in various database and they do not affect noticeably the phase behavior of their binary system. The influence of the organic compounds (*n*-alkane – cycloalkane – branched alkane) with the same number of carbon atoms (6) on the phase behavior of the binary systems was also discussed. For CCS applications, it seems that the carbon dioxide + cyclohexane binary system presents the best potential, followed by the carbon dioxide + *n*-hexane and finally by carbon dioxide + 2,3-dimethylbutane.

AUTHOR INFORMATION

Corresponding Authors
*E-mails: catinca.secuianu@upb.ro (C.S.); dnichita@univ-pau.fr (D.V.N.)

ORCID
Catinca Secuianu: 0000-0001-5779-6415
Sergiu Sima: 0000-0002-4789-7287
Dan Vladimir Nichita: 0000-0002-5558-7617

Notes
The authors declare no competing financial interest.

ACKNOWLEDGMENTS

„This work was supported by a grant of Ministry of Research, Innovation, and Digitization, CNCS - UEFISCDI, project number PN-III-P4-PCE-2021-0717, within PNCDI III”.

ASSOCIATED CONTENT

Supporting Information.

Analysis of experimental literature data (**Figures 1S** to **9S**) and description of GEOS, PR, and SRK cubic equations of state together the comparisons of experimental data and modeling results (**Figures 11S** to **26S**).

REFERENCES

(1) Dohrn, R.; Brunner, G. High-pressure fluid-phase equilibria: Experimental methods and systems investigated (1988–1993). *Fluid Phase Equilibria* **1995**, *106* (1), 213-282. DOI: https://doi.org/10.1016/0378-3812(95)02703-H.
(2) Christov, M.; Dohrn, R. High-pressure fluid phase equilibria: Experimental methods and systems investigated (1994–1999). *Fluid Phase Equilibria* **2002**, *202* (1), 153-218. DOI: https://doi.org/10.1016/S0378-3812(02)00096-1.
(3) Dohrn, R.; Peper, S.; Fonseca, J. M. S. High-pressure fluid-phase equilibria: Experimental methods and systems investigated (2000–2004). *Fluid Phase Equilibria* **2010**, *288* (1), 1-54. DOI: https://doi.org/10.1016/j.fluid.2009.08.008.
(4) Fonseca, J. M. S.; Dohrn, R.; Peper, S. High-pressure fluid-phase equilibria: Experimental methods and systems investigated (2005–2008). *Fluid Phase Equilibria* **2011**, *300* (1), 1-69. DOI: https://doi.org/10.1016/j.fluid.2010.09.017.
(5) Peper, S.; Fonseca, J. M. S.; Dohrn, R. High-pressure fluid-phase equilibria: Trends, recent developments, and systems investigated (2009–2012). *Fluid Phase Equilibria* **2019**, *484*, 126-224. DOI: https://doi.org/10.1016/j.fluid.2018.10.007.
(6) Dohrn, R.; Peper, S.; Secuianu, C.; Fonseca, J. M. S. High-pressure fluid-phase equilibria: Experimental methods, developments and systems investigated (2013–2016). *Fluid Phase Equilibria* **2024**, *579*, 113978. DOI: https://doi.org/10.1016/j.fluid.2023.113978.
(7) Wei, C.; Zhang, W.; Yang, K.; Bai, X.; Xu, S.; Li, J.; Liu, Z. An efficient way to use CO2 as chemical feedstock by coupling with alkanes. *Chinese Journal of Catalysis* **2023**, *47*, 138-149. DOI: https://doi.org/10.1016/S1872-2067(23)64416-X.
(8) Zhang, Z.; Song, Z.; Hao, H.; Huang, L.; Song, Y. Adsorption behavior of n-hexane and its mixtures with CO2, CH4, H2O and SDBS in hydrophobic silica nanopores. *Fuel* **2022**, *312*, 122872. DOI: https://doi.org/10.1016/j.fuel.2021.122872.
(9) Vega, F.; Baena-Moreno, F. M.; Gallego Fernández, L. M.; Portillo, E.; Navarrete, B.; Zhang, Z. Current status of CO2 chemical absorption research applied to CCS: Towards full deployment at industrial scale. *Applied Energy* **2020**, *260*, 114313. DOI: https://doi.org/10.1016/j.apenergy.2019.114313.
(10) Al Ghafri, S. Z.; Maitland, G. C.; Trusler, J. P. M. Experimental and modeling study of the phase behavior of synthetic crude oil+CO2. *Fluid Phase Equilibria* **2014**, *365*, 20-40. DOI: https://doi.org/10.1016/j.fluid.2013.12.018.
(11) Eller, F. J.; Taylor, S. L.; Curren, M. S. S. Use of liquid carbon dioxide to remove hexane from soybean oil. *Journal of the American Oil Chemists' Society* **2004**, *81* (10), 989-992. DOI: 10.1007/s11746-004-1011-7.
(12) Okajima, I.; Ito, K.; Aoki, Y.; Kong, C. Y.; Sako, T. Extraction of Rice Bran Oil Using CO2-Expanded Hexane in the Two-Phase Region. *Energies* **2022**, *15* (7), 2594. DOI: https://doi.org/10.3390/en15072594.
(13) Yeddes, N.; Chérif, J. K.; Jrad, A.; Barth, D.; Trabelsi-Ayadi, M. Supercritical SC-CO(2) and Soxhlet n-Hexane Extract of Tunisian Opuntia ficus indica Seeds and Fatty Acids Analysis. *J Lipids* **2012**, *2012*, 914693. DOI: 10.1155/2012/914693 From NLM.
(14) Đurđević, S.; Milovanović, S.; Šavikin, K.; Ristić, M.; Menković, N.; Pljevljakušić, D.; Petrović, S.; Bogdanović, A. Improvement of supercritical CO2 and n-hexane extraction of wild growing pomegranate seed oil by microwave pretreatment. *Industrial Crops and Products* **2017**, *104*, 21-27. DOI: https://doi.org/10.1016/j.indcrop.2017.04.024.

(15) Koller, T. M.; Yan, S.; Steininger, C.; Klein, T.; Fröba, A. P. Interfacial Tension and Liquid Viscosity of Binary Mixtures of n-Hexane, n-Decane, or 1-Hexanol with Carbon Dioxide by Molecular Dynamics Simulations and Surface Light Scattering. *International Journal of Thermophysics* **2019**, *40* (8), 79. DOI: 10.1007/s10765-019-2544-y.
(16) Moreau, A.; Polishuk, I.; Segovia, J. J.; Tuma, D.; Vega-Maza, D.; Martín, M. C. Measurements and predictions of densities and viscosities in CO2 + hydrocarbon mixtures at high pressures and temperatures: CO2 + n-pentane and CO2 + n-hexane blends. *Journal of Molecular Liquids* **2022**, *360*, 119518. DOI: https://doi.org/10.1016/j.molliq.2022.119518.
(17) Meylan, F. D.; Moreau, V.; Erkman, S. CO2 utilization in the perspective of industrial ecology, an overview. *Journal of CO2 Utilization* **2015**, *12*, 101-108. DOI: https://doi.org/10.1016/j.jcou.2015.05.003.
(18) Macawile, M. C.; Auresenia, J. Utilization of Supercritical Carbon Dioxide and Co-solvent n-hexane to Optimize Oil Extraction from Gliricidia sepium Seeds for Biodiesel Production. *Applied Science and Engineering Progress* **2021**, *15* (1). DOI: 10.14416/j.asep.2021.09.003 (acccessed 2024/05/01).
(19) Monteagudo-Olivan, R.; Cocero, M. J.; Coronas, J.; Rodríguez-Rojo, S. Supercritical CO2 encapsulation of bioactive molecules in carboxylate based MOFs. *Journal of CO2 Utilization* **2019**, *30*, 38-47. DOI: https://doi.org/10.1016/j.jcou.2018.12.022.
(20) Matsuyama, K.; Hayashi, N.; Yokomizo, M.; Kato, T.; Ohara, K.; Okuyama, T. Supercritical carbon dioxide-assisted drug loading and release from biocompatible porous metal–organic frameworks. *Journal of Materials Chemistry B* **2014**, *2* (43), 7551-7558, 10.1039/C4TB00725E. DOI: 10.1039/C4TB00725E.
(21) Feng, Y.; Meier, D. Comparison of supercritical CO2, liquid CO2, and solvent extraction of chemicals from a commercial slow pyrolysis liquid of beech wood. *Biomass and Bioenergy* **2016**, *85*, 346-354. DOI: https://doi.org/10.1016/j.biombioe.2015.12.027.
(22) Jacques, R. A.; Santos, J. G.; Dariva, C.; Oliveira, J. V.; Caramão, E. B. GC/MS characterization of mate tea leaves extracts obtained from high-pressure CO2 extraction. *The Journal of Supercritical Fluids* **2007**, *40* (3), 354-359. DOI: https://doi.org/10.1016/j.supflu.2006.07.023.
(23) Nelson, W. M.; Naidoo, P.; Ramjugernath, D. A new high pressure phase equilibrium cell featuring the static-combined method: Equipment commissioning and data measurement. *The Journal of Supercritical Fluids* **2021**, *176*, 105291. DOI: https://doi.org/10.1016/j.supflu.2021.105291.
(24) Hassanalizadeh, R.; Nelson, W. M.; Naidoo, P.; Mohammadi, A. H.; Negadi, L.; Ramjugernath, D. VLE measurements and modelling for the binary systems of (CF4 + C6F14) and (CF4+ C8F18). *Fluid Phase Equilibria* **2019**, *485*, 146-152. DOI: https://doi.org/10.1016/j.fluid.2018.12.005.
(25) Ebrahiminejadhasanabadi, M.; Nelson, W. M.; Naidoo, P.; Mohammadi, A. H.; Ramjugernath, D. Experimental measurement of carbon dioxide solubility in 1-methylpyrrolidin-2-one (NMP) + 1-butyl-3-methyl-1H-imidazol-3-ium tetrafluoroborate ([bmim][BF4]) mixtures using a new static-synthetic cell. *Fluid Phase Equilibria* **2018**, *477*, 62-77. DOI: https://doi.org/10.1016/j.fluid.2018.08.017.
(26) Nelson, W. M.; Ramjugernath, D. Experimental Solubility Data for Binary Mixtures of Ethane and 2,2,4-Trimethylpentane at Pressures up to 6 MPa Using a New Variable-Volume Sapphire Cell. *Journal of Chemical & Engineering Data* **2017**, *62* (11), 3915-3920. DOI: 10.1021/acs.jced.7b00613.

(27) Williams-Wynn, M. D.; Naidoo, P.; Ramjugernath, D. Isothermal (vapour+liquid) equilibrium data for binary systems of (n-hexane+CO2 or CHF3). *The Journal of Chemical Thermodynamics* **2016**, *94*, 31-42. DOI: https://doi.org/10.1016/j.jct.2015.10.009.
(28) Zhu, R. Y., J.; Xu, W.; Liu, Z.; Tian, Y. High pressure vapor-liquid equilibrium of carbon dioxide-hexane system. *Huagong Xuebao / Journal of Chemical Industry and Engineering (China)* **2006**, *57* (10), 2270-2277.
(29) Yu, J. T., Y.; Zhu, R.; Liu, Z. High pressure vapor-liquid equilibrium of supercritical carbon dioxide + n-hexane system. *Trans. Tianjin Univ.* **2006** *12* (6), 452-456.
(30) DETHERM Database. DECHEMA Chemistry Data Series. (accessed.
(31) Han, H.; Yuan, S.; Li, S.; Liu, X.; Chen, X. Dissolving capacity and volume expansion of carbon dioxide in chain n-alkanes. *Petroleum Exploration and Development* **2015**, *42* (1), 97-103. DOI: https://doi.org/10.1016/S1876-3804(15)60011-8.
(32) King, M. B.; Al-Najjar, H. The solubilities of carbon dioxide, hydrogen sulphide and propane in some normal alkane solvents—I: Experimental determinations in the range 15–70°C and comparison with ideal solution values. *Chemical Engineering Science* **1977**, *32* (10), 1241-1246. DOI: https://doi.org/10.1016/0009-2509(77)80059-6.
(33) Choi, E.-J.; Yeo, S.-D. Critical Properties for Carbon Dioxide + n-Alkane Mixtures Using a Variable-Volume View Cell. *Journal of Chemical & Engineering Data* **1998**, *43* (5), 714-716. DOI: 10.1021/je9800297.
(34) Ziegler, J. W.; Chester, T. L.; Innis, D. P.; Page, S. H.; Dorsey, J. G. Supercritical Fluid Flow Injection Method for Mapping Liquid—Vapor Critical Loci of Binary Mixtures Containing CO₂. In *Innovations in Supercritical Fluids*, ACS Symposium Series, Vol. 608; American Chemical Society, 1995; pp 93-110.
(35) Ziegler, J. W.; Dorsey, J. G.; Chester, T. L.; Innis, D. P. Estimation of Liquid-Vapor Critical Loci for CO2-Solvent Mixtures Using a Peak-Shape Method. *Analytical Chemistry* **1995**, *67* (2), 456-461. DOI: 10.1021/ac00098a034.
(36) Leder, F.; Irani, C. A. Upper critical solution temperatures in carbon dioxide-hydrocarbon systems. *Journal of Chemical & Engineering Data* **1975**, *20* (3), 323-327. DOI: 10.1021/je60066a019.
(37) Gurdial, G. S.; Foster, N. R.; Yun, S. L. J.; Tilly, K. D. Phase Behavior of Supercritical Fluid—Entrainer Systems. In *Supercritical Fluid Engineering Science*, ACS Symposium Series, Vol. 514; American Chemical Society, 1992; pp 34-45.
(38) Liu, J.; Qin, Z.; Wang, G.; Hou, X.; Wang, J. Critical Properties of Binary and Ternary Mixtures of Hexane + Methanol, Hexane + Carbon Dioxide, Methanol + Carbon Dioxide, and Hexane + Carbon Dioxide + Methanol. *Journal of Chemical & Engineering Data* **2003**, *48* (6), 1610-1613. DOI: 10.1021/je034127q.
(39) Sun, Y.; Li, Y.; Zhou, J.; Zhu, R.; Tian, Y. Experimental determination and calculation of the critical curves for the binary systems of CO2 containing ketone, alkane, ester and alcohol, respectively. *Fluid Phase Equilibria* **2011**, *307* (1), 72-77. DOI: https://doi.org/10.1016/j.fluid.2011.05.005.
(40) Im, U. K.; Kurata, F. Heterogeneous phase behavior of carbon dioxide in n-hexane and n-heptane at low temperatures. *Journal of Chemical & Engineering Data* **1971**, *16* (4), 412-415. DOI: 10.1021/je60051a011.
(41) van Konynenburg, P. H.; Scott, R. L.; Rowlinson, J. S. Critical lines and phase equilibria in binary van der Waals mixtures. *Philosophical Transactions of the Royal Society of London.*

Series A, Mathematical and Physical Sciences **1980**, *298* (1442), 495-540. DOI: 10.1098/rsta.1980.0266 (acccessed 2021/01/06).
(42) Gainar, I. The solubility of CO2 and N2O in some C6 hydrocarbons at high pressures. *An. Univ. Bucuresti Chim.* **2003**, *12*, 197-202.
(43) Kaminishi, G.-I.; Yokoyama, C.; Shinji, T. Vapor pressures of binary mixtures of carbon dioxide with benzene, n-hexane and cyclohexane up to 7 MPa. *Fluid Phase Equilibria* **1987**, *34* (1), 83-99. DOI: https://doi.org/10.1016/0378-3812(87)85052-5.
(44) Ohgaki, K.; Katayama, T. Isothermal vapor-liquid equilibrium data for binary systems containing carbon dioxide at high pressures: methanol-carbon dioxide, n-hexane-carbon dioxide, and benzene-carbon dioxide systems. *Journal of Chemical & Engineering Data* **1976**, *21* (1), 53-55. DOI: 10.1021/je60068a015.
(45) Liu, L.; He, J.; Gui, X. Measurement and correlation of solubility for alcohols and alkanes in ScCO2. *The Journal of Chemical Thermodynamics* **2022**, *171*, 106804. DOI: https://doi.org/10.1016/j.jct.2022.106804.
(46) Gui, X.; Wang, W.; Gao, Q.; Yun, Z.; Fan, M.; Chen, Z. Measurement and Correlation of High Pressure Phase Equilibria for CO2 + Alkanes and CO2 + Crude Oil Systems. *Journal of Chemical & Engineering Data* **2017**, *62* (11), 3807-3822. DOI: 10.1021/acs.jced.7b00517.
(47) Leal, M. F.; do Nascimento, F. P.; Paredes, M. L. L.; Pessoa, F. L. P. Experimental measurement and thermodynamic modeling of phase equilibria of {CO2 + tetralin + n-alkanes (with n=6, 16)} and its binary systems. *Fluid Phase Equilibria* **2018**, *478*, 23-33. DOI: https://doi.org/10.1016/j.fluid.2018.08.019.
(48) Yang, Z.; Li, M.; Peng, B.; Lin, M.; Dong, Z. Dispersion Property of CO2 in Oil. 1. Volume Expansion of CO2 + Alkane at near Critical and Supercritical Condition of CO2. *Journal of Chemical & Engineering Data* **2012**, *57* (3), 882-889. DOI: 10.1021/je201114g.
(49) Li, Y.-H.; Dillard, K. H.; Robinson, R. L., Jr. Vapor-liquid phase equilibrium for carbon dioxide-n-hexane at 40, 80, and 120 .degree.C. *Journal of Chemical & Engineering Data* **1981**, *26* (1), 53-55. DOI: 10.1021/je00023a018.
(50) Shenderei, E. R. I., F.P. Solubility of Carbon Dioxide in n-Hexane, n-Heptane and n-Octane at low Temperatures under Pressure. *Khim. Promst. Moscow* **1964**, *7*, 506-508.
(51) Lay, E. N.; Taghikhani, V.; Ghotbi, C. Measurement and Correlation of CO2 Solubility in the Systems of CO2 + Toluene, CO2 + Benzene, and CO2 + n-Hexane at Near-Critical and Supercritical Conditions. *Journal of Chemical & Engineering Data* **2006**, *51* (6), 2197-2200. DOI: 10.1021/je0602972.
(52) Lay, E. N. Measurement and Correlation of Bubble Point Pressure in (CO2 + C6H6), (CO2 + CH3C6H5), (CO2 + C6H14), and (CO2 + C7H16) at Temperatures from (293.15 to 313.15) K. *Journal of Chemical & Engineering Data* **2010**, *55* (1), 223-227. DOI: 10.1021/je900312z.
(53) Gao, Y.; Li, C.; Xia, S.; Ma, P. The solubility of CO2 in (hexane + cyclohexane) and (cyclopentane + ethylbenzene) and (toluene + undecane) systems at high pressures. *The Journal of Chemical Thermodynamics* **2021**, *154*, 106324. DOI: https://doi.org/10.1016/j.jct.2020.106324.
(54) Wagner, Z.; Wichterle, I. High-pressure vapour—liquid equilibrium in systems containing carbon dioxide, 1-hexene, and n-hexane. *Fluid Phase Equilibria* **1987**, *33* (1), 109-123. DOI: https://doi.org/10.1016/0378-3812(87)87006-1.
(55) Chen, D. C., W. Phase Behavior of n-Hexane and n-Octane in the Critical State Carbon Dioxide. *Huaxue Gongcheng Xi'an* **1992**, *20*, 66-69.

(56) Tolley, W. K. Supercritical behavior of selected metal chlorides with carbon dioxide: A study of solubilities, solution densities, and excess enthalpies of mixing. Master's Thesis, Brigham Young University, 1990.
(57) Wang, B.; Han, B.; Jiang, T.; Zhang, Z.; Xie, Y.; Li, W.; Wu, W. Enhancing the Rate of the Diels−Alder Reaction Using CO2 + Ethanol and CO2 + n-Hexane Mixed Solvents of Different Phase Regions. *The Journal of Physical Chemistry B* **2005**, *109* (50), 24203-24210. DOI: 10.1021/jp0553838.
(58) Wang, B.; He, J.; Sun, D.; Zhang, R.; Han, B. Solubility of chlorobutane, ethyl methacrylate and trifluoroethyl acrylate in supercritical carbon dioxide. *Fluid Phase Equilibria* **2006**, *239* (1), 63-68. DOI: https://doi.org/10.1016/j.fluid.2005.10.023.
(59) Shi, Q.; Jing, L.; Qiao, W. Solubility of n-alkanes in supercritical CO2 at diverse temperature and pressure. *Journal of CO2 Utilization* **2015**, *9*, 29-38. DOI: https://doi.org/10.1016/j.jcou.2014.12.002.
(60) Geana, D. New equation of state for fluids. 1. Application to PVTcalculi for pure fluids. *Revista de Chimie* **1986**, *37* (5), 303-309, Article.
(61) Geana, D. New fluid state equation. 2. Application to the phase equilibrium calculus. *Revista de Chimie* **1986**, *37* (11), 951-959, Article.
(62) Geana, D. New state equation for fluids. 3. Generalization of the cubic equations of state of the van der Waals type. *Revista de Chimie* **1987**, *38* (11), 975-979, Article.
(63) Peng, D. Y.; Robinson, D. B. A New Two-Constant Equation of State. *Industrial and Engineering Chemistry Fundamentals* **1976**, *15* (1), 59-64, Article. DOI: 10.1021/i160057a011 Scopus.
(64) Soave, G. Equilibrium constants from a modified Redlich-Kwong equation of state. *Chemical Engineering Science* **1972**, *27* (6), 1197-1203, Article. DOI: 10.1016/0009-2509(72)80096-4 Scopus.
(65) Jaubert, J.-N.; Mutelet, F. VLE predictions with the Peng–Robinson equation of state and temperature dependent kij calculated through a group contribution method. *Fluid Phase Equilibria* **2004**, *224* (2), 285-304. DOI: https://doi.org/10.1016/j.fluid.2004.06.059.
(66) Mutelet, F.; Vitu, S.; Privat, R.; Jaubert, J.-N. Solubility of CO2 in branched alkanes in order to extend the PPR78 model (predictive 1978, Peng–Robinson EOS with temperature-dependent kij calculated through a group contribution method) to such systems. *Fluid Phase Equilibria* **2005**, *238* (2), 157-168. DOI: https://doi.org/10.1016/j.fluid.2005.10.001.
(67) Vitu, S.; Privat, R.; Jaubert, J.-N.; Mutelet, F. Predicting the phase equilibria of CO2+hydrocarbon systems with the PPR78 model (PR EOS and kij calculated through a group contribution method). *The Journal of Supercritical Fluids* **2008**, *45* (1), 1-26. DOI: https://doi.org/10.1016/j.supflu.2007.11.015.
(68) Privat, R.; Jaubert, J.-N. The state of the art of cubic equations of state with temperature-dependent binary interaction coefficients: From correlation to prediction. *Fluid Phase Equilibria* **2023**, *567*, 113697. DOI: https://doi.org/10.1016/j.fluid.2022.113697.
(69) Design Institute for Physical Properties, S. b. A. DIPPR Project 801 - Full Version. Design Institute for Physical Property Research/AIChE.
(70) Poling, B. E. P., John M.; O'Connell, John P.; Reid, Robert C. *The Properties of Gases and Liquids*; McGraw-Hill Education, 2000.
(71) Reid, R. C. P., J. M.; Poling, B. E. *The Properties of Gases and Liquids, 4th Edition*; McGraw-Hill, Inc., 1987.

(72) Sima, S.; Secuianu, C. The Effect of Functional Groups on the Phase Behavior of Carbon Dioxide Binaries and Their Role in CCS. *Molecules* **2021**, *26* (12), 3733. DOI: https://doi.org/10.3390/molecules26123733.
(73) Sima, S.; Crişciu, A. V.; Secuianu, C. Phase Behavior of Carbon Dioxide + Isobutanol and Carbon Dioxide + tert-Butanol Binary Systems. *Energies* **2022**, *15* (7), 2625. DOI: https://doi.org/10.3390/en15072625
(74) Sima, S.; Cruz-Doblas, J.; Cismondi, M.; Secuianu, C. High-pressure phase equilibrium calculations for carbon dioxide + cyclopentane binary system. *Central European Journal of Chemistry* **2014**, *12* (9), 918-927, Article. DOI: 10.2478/s11532-013-0393-2 Scopus.
(75) Sima, S.; Milanesio, J. M.; Ramello, J. I.; Cismondi, M.; Secuianu, C.; Feroiu, V.; Geană, D. The effect of the naphthenic ring on the VLE of (carbon dioxide+alkane) mixtures. *The Journal of Chemical Thermodynamics* **2016**, *93*, 374-385. DOI: https://doi.org/10.1016/j.jct.2015.07.018.
(76) Ioniţă, M.; Sima, S.; Crişciu, A.; Secuianu, C.; Nichita, D. V. Phase behavior of carbon dioxide + 2,4-dimethylpentane binary system at high pressures. *The Journal of Supercritical Fluids* **2023**, *199*, 105941. DOI: https://doi.org/10.1016/j.supflu.2023.105941.
(77) Guilbot, P.; Valtz, A.; Legendre, H.; Richon, D. Rapid on-line sampler-injector: a reliable tool for HT-HP sampling and on-line GC analysis. *Analusis* **2000**, *28* (5), 426-431. DOI: https://doi.org/10.1051/analusis:2000128.
(78) Peper, S.; Dohrn, R. Sampling from fluid mixtures under high pressure: Review, case study and evaluation. *The Journal of Supercritical Fluids* **2012**, *66*, 2-15. DOI: https://doi.org/10.1016/j.supflu.2011.09.021.
(79) Sima, S.; Secuianu, C.; Nichita, D. V. High-pressure phase equilibria of carbon dioxide + 1,4-dioxane binary system. *Fluid Phase Equilibria* **2021**, *547*, 113181. DOI: https://doi.org/10.1016/j.fluid.2021.113181.
(80) Sima, S.; Cismondi, M.; Secuianu, C. High-Pressure Phase Equilibrium for Carbon Dioxide + Ethyl n-Butyrate Binary System. *Journal of Chemical & Engineering Data* **2021**, *66* (11), 4094-4102. DOI: 10.1021/acs.jced.1c00319.
(81) Sima, S. I., Mihaela; Secuianu, Catinca. Phase equilibria of carbon dioxide + 2,4-dimethylpentane. In 31st European Symposium on Applied Thermodynamics – 5-9 July 2021, Paris, France (virtual); 2021.
(82) Ioniţă, M. S., S.; Cismondi, M.; Secuianu, C. Phase equilibria for the carbon dioxide + cyclopentane + cyclohexane system at high pressures. *Rev. Roum. Chim.* **2021**, *66* (3), 303-308. DOI: 10.33224/rrch.2021.66.3.11.
(83) Tiwikrama, A. H.; Afrianto; Chiu, H. Y.; Peng, D. Y.; Lin, H. M.; Lee, M. J. Vapour-liquid phase boundaries including the near critical regions of the (CO2 + styrene, CO2 + 1,4-dioxane, and CO2 + N,N-dimethylformamide)systems. *Journal of Chemical Thermodynamics* **2019**, *136*, 141-148, Article. DOI: 10.1016/j.jct.2019.05.004 Scopus.
(84) Piña-Martinez, A.; Privat, R.; Jaubert, J.-N. Use of 300,000 pseudo-experimental data over 1800 pure fluids to assess the performance of four cubic equations of state: SRK, PR, tc-RK, and tc-PR. *AIChE Journal* **2022**, *68* (2), e17518. DOI: https://doi.org/10.1002/aic.17518.
(85) Ionita, M. C., Adrian V.; Racovita, Radu C.; Sima, Sergiu; Secuianu, Catinca. Phase diagram predictions for carbon dioxide + different classes of organic substances at high pressures.

University Politehnica of Bucharest Scientific Bulletin Series B-Chemistry and Materials Science **2021**, *83* (2), 117-132.

(86) Secuianu, C.; Feroiu, V.; Geană, D. Phase behavior for the carbon dioxide + 2-butanol system: Experimental measurements and modeling with cubic equations of state. *Journal of Chemical and Engineering Data* **2009**, *54* (5), 1493-1499, Article. DOI: 10.1021/je800799n Scopus.
(87) Crisciu, A.; Sima, S.; Deaconu, A. S.; Chirila, A.; Deaconu, D.; Secuianu, C.; Feroiu, V. Modelling of the carbon dioxide + cyclohexane binary system with cubic equations of state. *Revista de Chimie* **2016**, *67* (10), 1984-1989, Article. Scopus.

(88) Zhang, R.; Qin, Z.; Wang, G.; Dong, M.; Hou, X.; Wang, J. Critical Properties of the Reacting Mixture in the Selective Oxidation of Cyclohexane by Oxygen in the Presence of Carbon Dioxide. *Journal of Chemical & Engineering Data* **2005**, *50* (4), 1414-1418. DOI: 10.1021/je0500882.
(89) Sima, S. C., Adrian V.; Secuianu, Catinca; Nichita, Dan Vladimir. High-pressure phase equilibria for carbon dioxide + 2,3-dimethylbutane. *Fluid Phase Equilib.* **2024**, *to be submitted*.